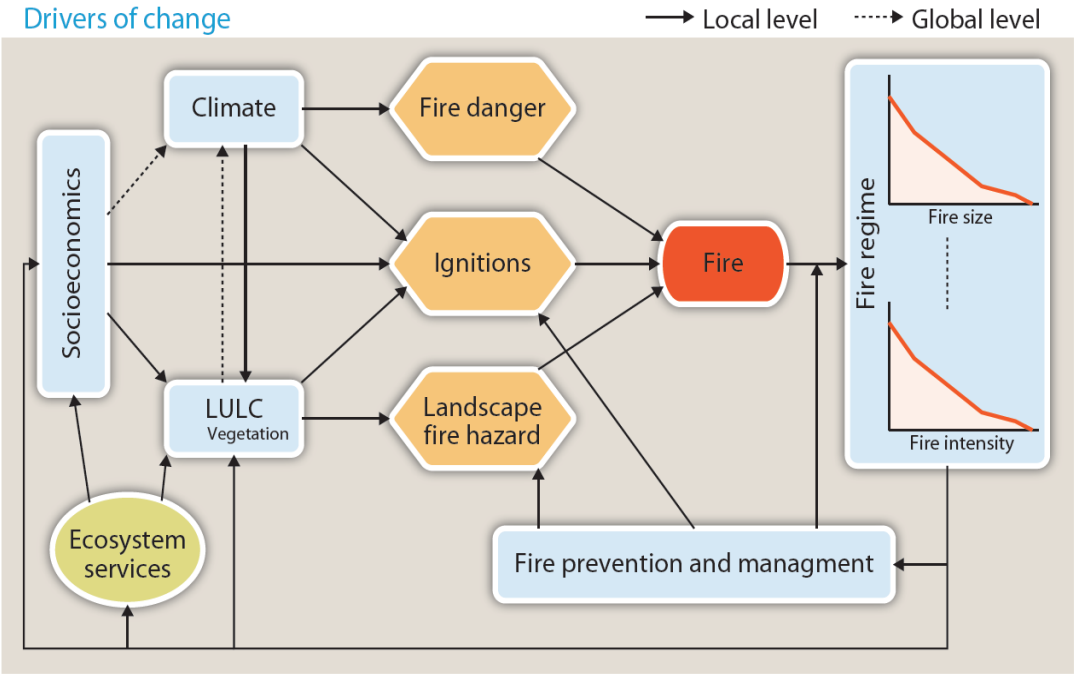

Figure 1. Diagram showing the complex interactions among the various factors that affect forest fires. Socioeconomic drivers affect the global economy and, through it, the global and local climate and land use and land cover (LULC). These determine fire danger, ignition sources and fire hazard. Fire spread will depend on fire fighting and other management measures. Fire regime is the result of these interacting factors. Fires can modify the landscape and affect future fires as well as ecosystem services. Changes in drivers will affect fire regime.

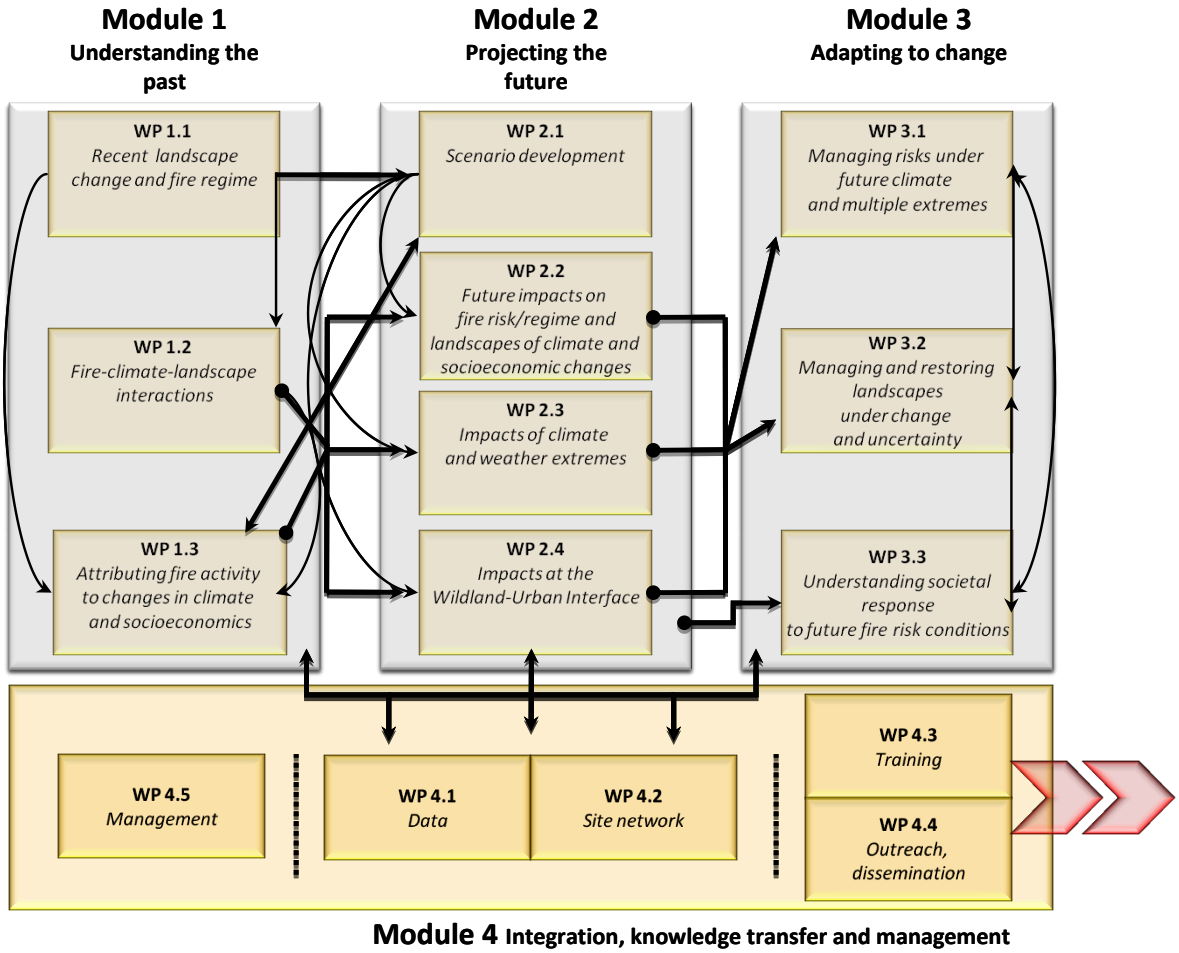

Figure 2. Operational structure of FUME and interlinks between work packages.

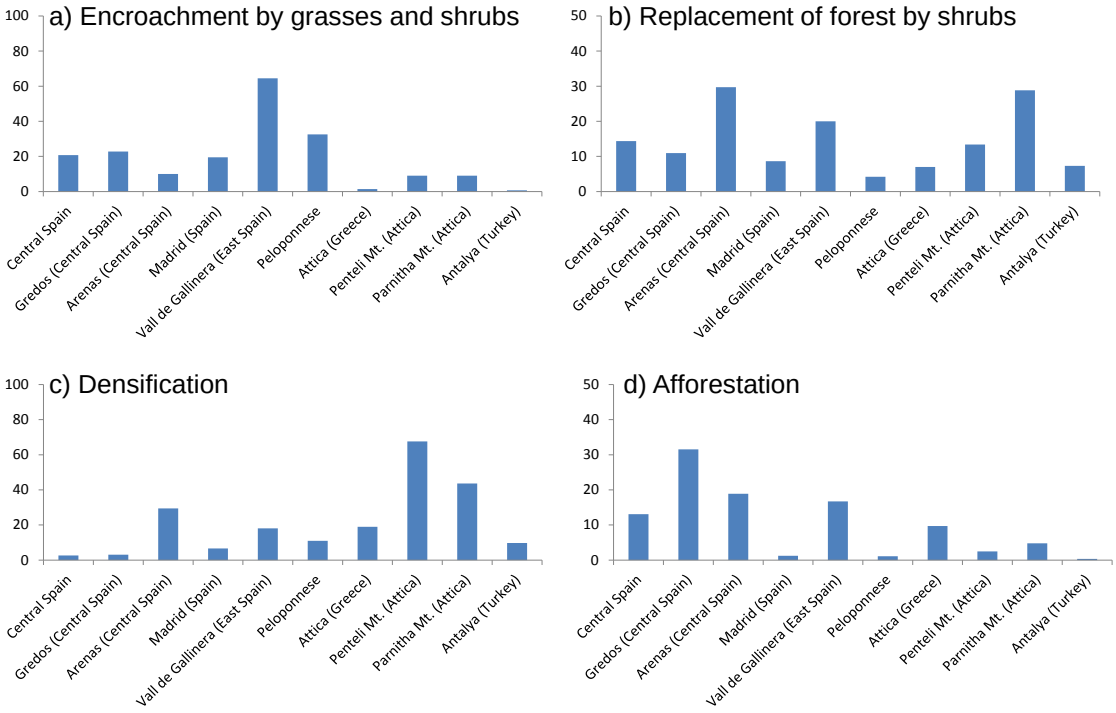

Figure 3. Percentage of LULC change at the various sites by processes related to: a) land abandonment (encroachment by grasses and shrubs), b) shrublands invasion caused by fires, c) densification of transitional [i.e., open] woodlands and shrublands, and d) afforestation before 1990´s.

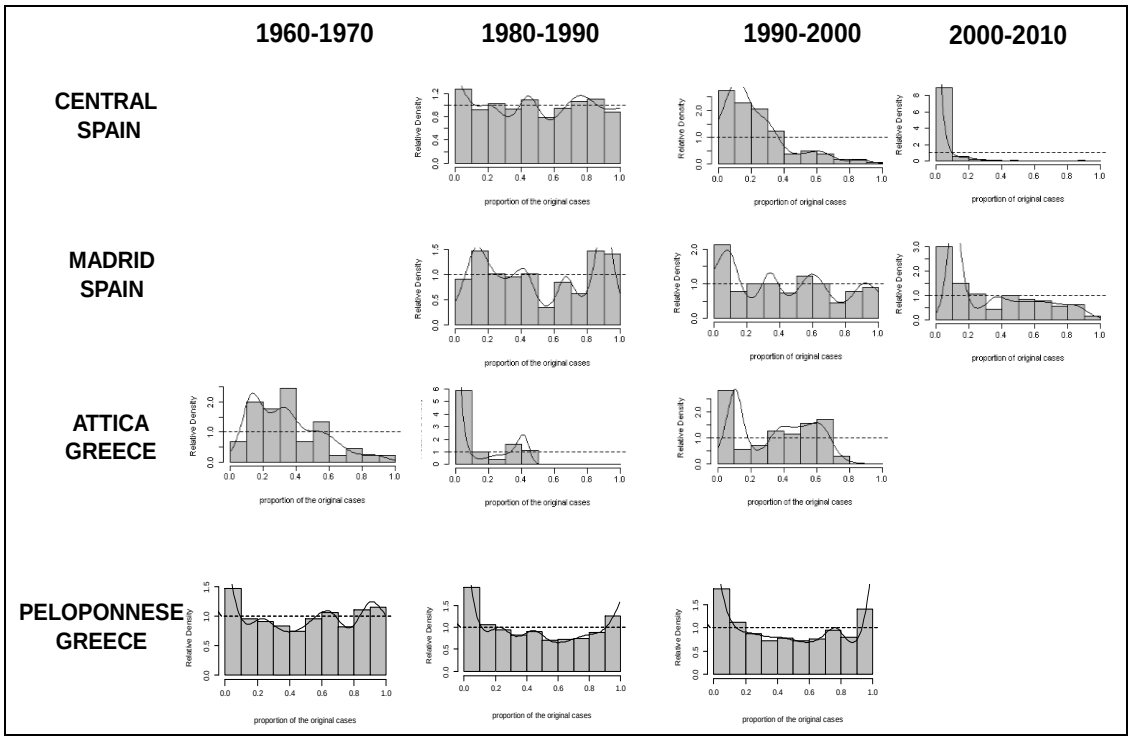

Figure 4. Relative distribution functions of livestock density between pair of dates in several study areas of FUME project.

Figure 5. Temporal evolution of annual number of fires and burned area in EU-Med by share (in %) of fire size categories (data elaborated from the European Fire Database of EFFIS, San Miguel-Ayanz et al., 2012; Assessing Hazards, Emergencies and Disaster Impacts. InTech,: 87-105). Note the increasing trend in the number of small fires, likely due to the variation of recording and reporting systems throughout the period considered.

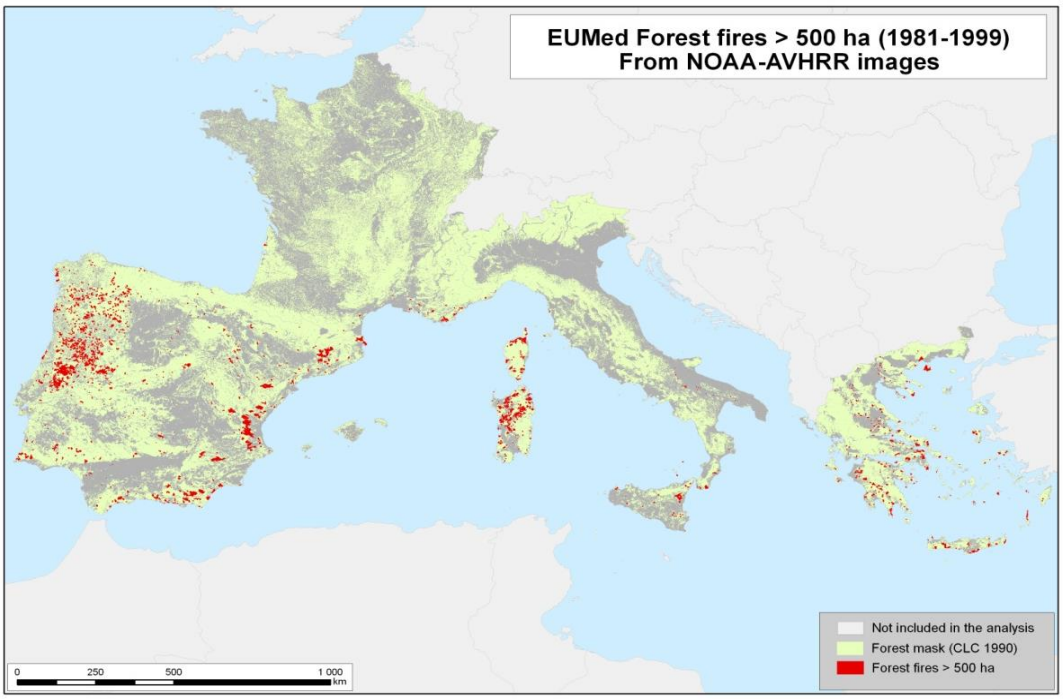

Figure 6. Forest fires >500ha in Mediterranean Europe obtained from NOAA-AVHRR images (1981-1999).

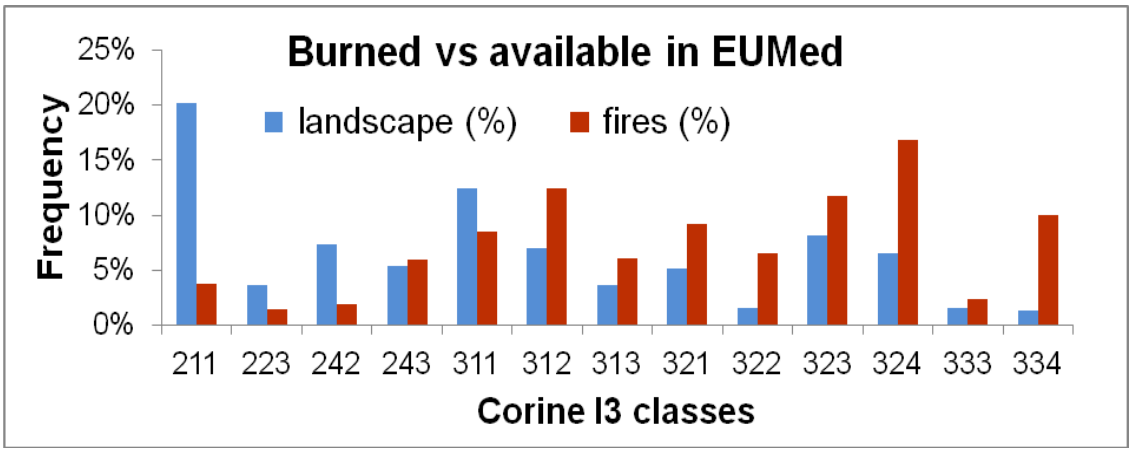

211	Non-irrigated arable land	321	Natural grassland
223	Olive groves	322	Moors and heathland
242	Complex cultivation patterns	323	Sclerophyllous vegetation
311	Broad-leaved forest	324	Transitional woodland shrub
312	Coniferous forest	333	Sparsely vegetated areas
313	Mixed forest	334	Burned areas
243	Land principally occupied by agriculture, with significant areas of natural vegetation		

Figure 7. Fire selectivity results for various LULC types in the Mediterranean Europe. Selectivity is shown when fires burn more (positive selectivity) or less (negative selectivity) (fires %) than what it is available (landscape %) in the territory.

Figure 8. The RUImap tool.

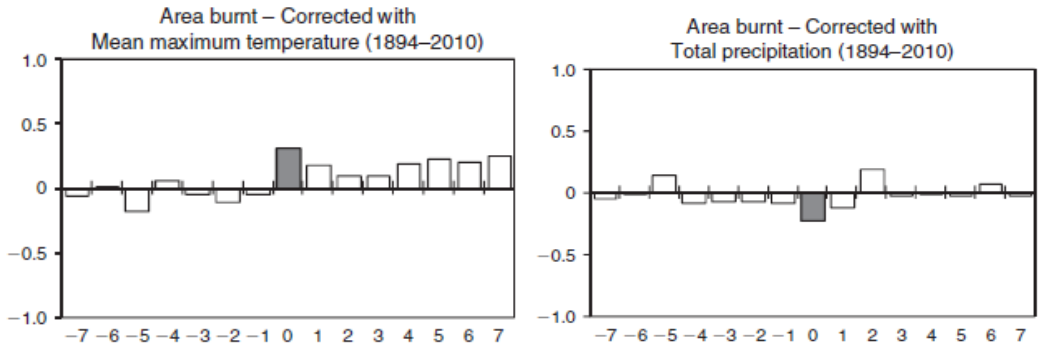

Figure 9. Cross-correlation between corrected area burnt and mean maximum temperature and precipitation in Greece for the period 1894–2010 (grey columns indicate significant values at 95% confidence level) (modified from Koutsias et al. 2013; International Journal of Wildland Fire 22: 493–507).

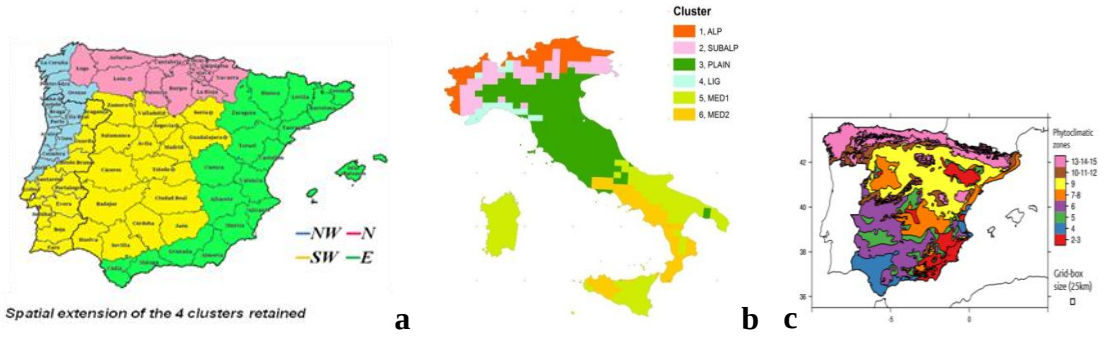

Figure 10. Examples of homogeneous units in terms of climate, fuel type characteristics, and fire occurrence used for the analysis in task 1.2.1. a) Spatial extension of the four clusters obtained for the normalized burnt area in the 66 administrative regions (AR) of Iberia (Trigo et al., 2013; International Journal of Climatology, doi: 10.1002/joc.3749.). b) Spatial extension of the six clusters obtained after hierarchical analysis in Italy. c) Spanish different phytoclimatic areas after aggregation (Bedia et al., 2013; Climate Change, 120: 1431-1441).

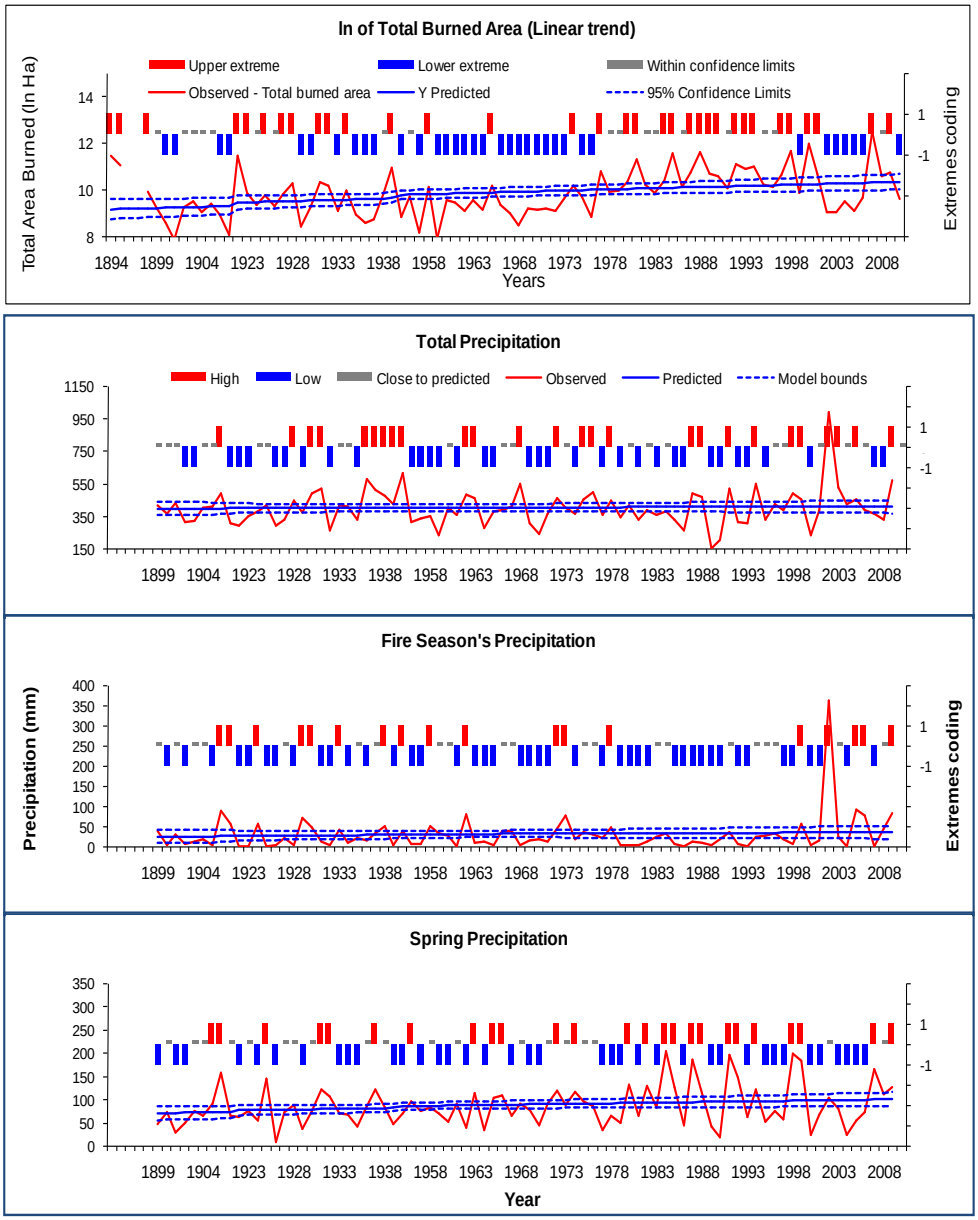

Figure 11. Trend lines and the 95% confidence intervals of the trend line of fire occurrence statistics (burned area) and the trend line of precipitation related meteorological parameters (total, spring and fire season precipitation). These are used as bounds to define strongly positive (red columns), strongly negative (blue columns), and close-to-predicted (grey columns) values of fire occurrence (modified from Xystrakis et al., 2013; Natural Hazards and Earth System Sciences, 1 (2): 693-720).

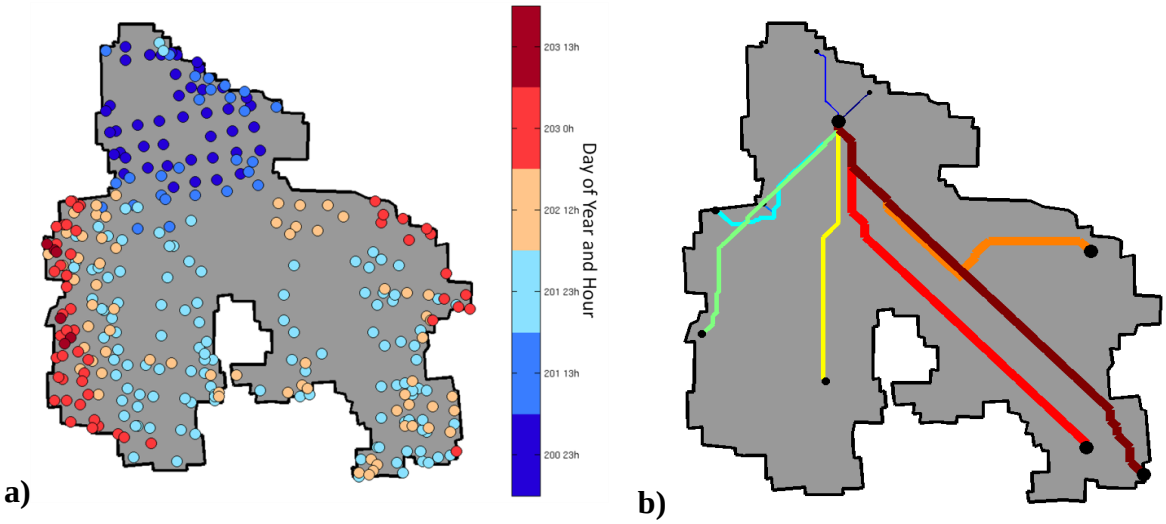

Figure 12. Spatial and temporal distribution of a) wildfire spread and b) the major fire paths in a reconstruction of a large fire in Portugal.

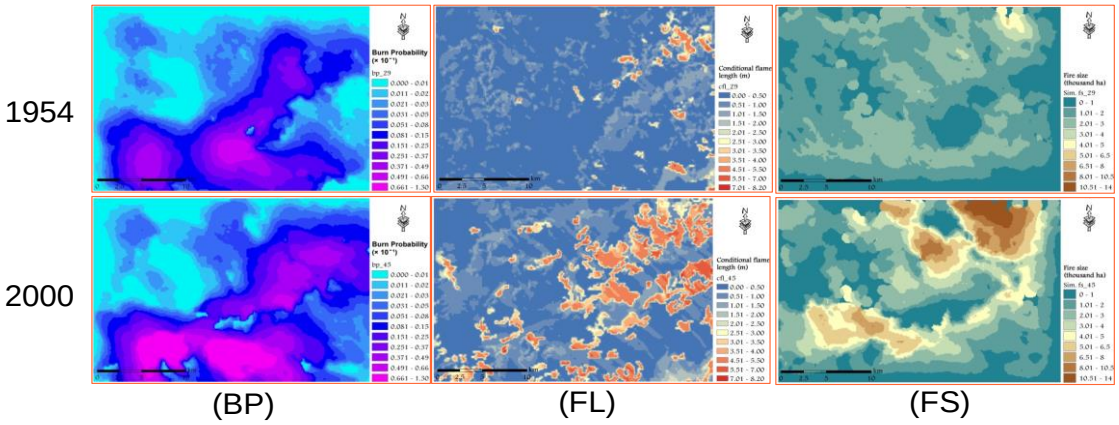

Figure 13. Nuoro study site. Maps of burn probability (BP), flame length (FL), and fire size (FS) considering fuel model maps of 1954 and 2000. Simulations run holding constant wind speed (35 kmh^{-1}) and direction (315°), fuel moisture (extreme), and historical ignitions pattern.

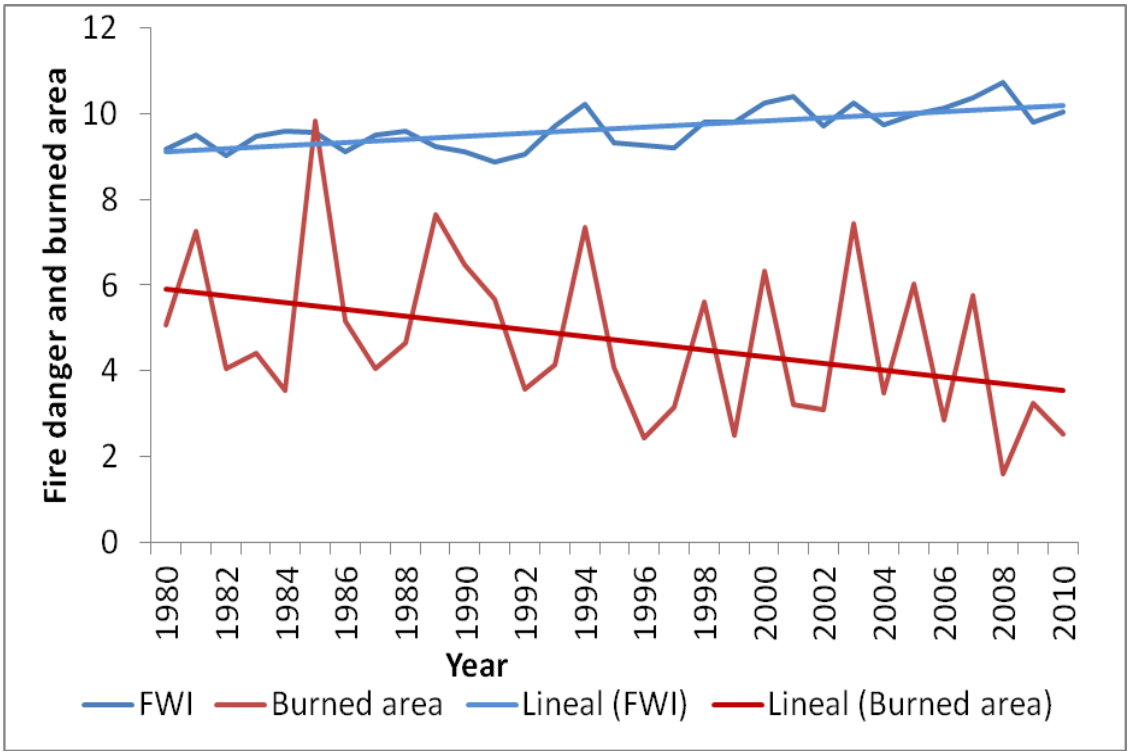

Figure 14. Total burned area (red line) in the Mediterranean countries (Greece, France, Italy, Spain, Portugal) and March-September mean FWI (blue line) calculated using ERA Interim dataset.

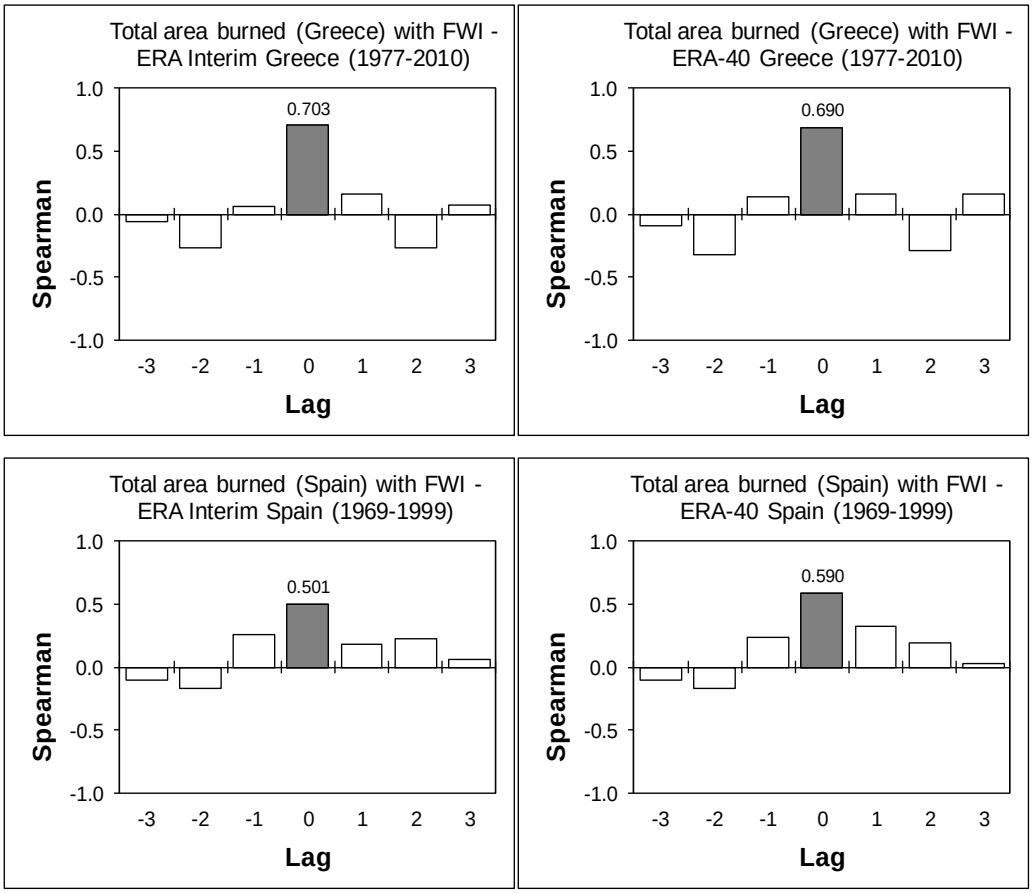

Figure 15. Cross-correlation graphs between total burned area at national scale in Greece and Spain and FWI values estimated from ERA Interim and ERA-40 data for homogeneous periods. Gray columns indicate significant values at 95% confidence level, indicating positive correlation between FWI and burned area.

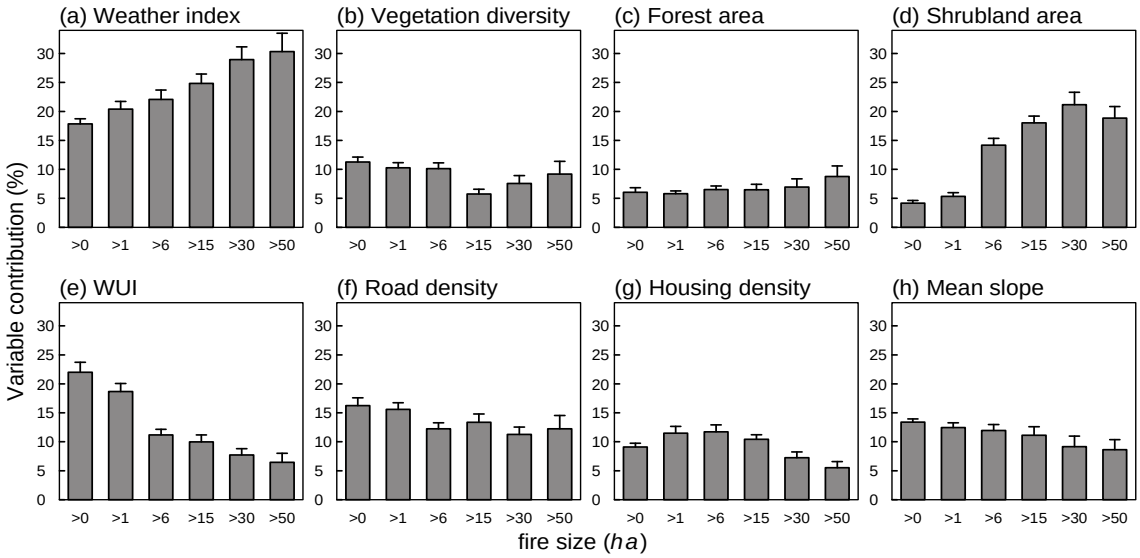

Figure 16. Relative contribution of weather, vegetation diversity, forest cover, shrubland cover, wildland urban interface (WUI), road density, housing density and slope to fire hazard for fire sizes varying between ignitions and fires larger than 50ha at Languedoc-Roussillon (France).

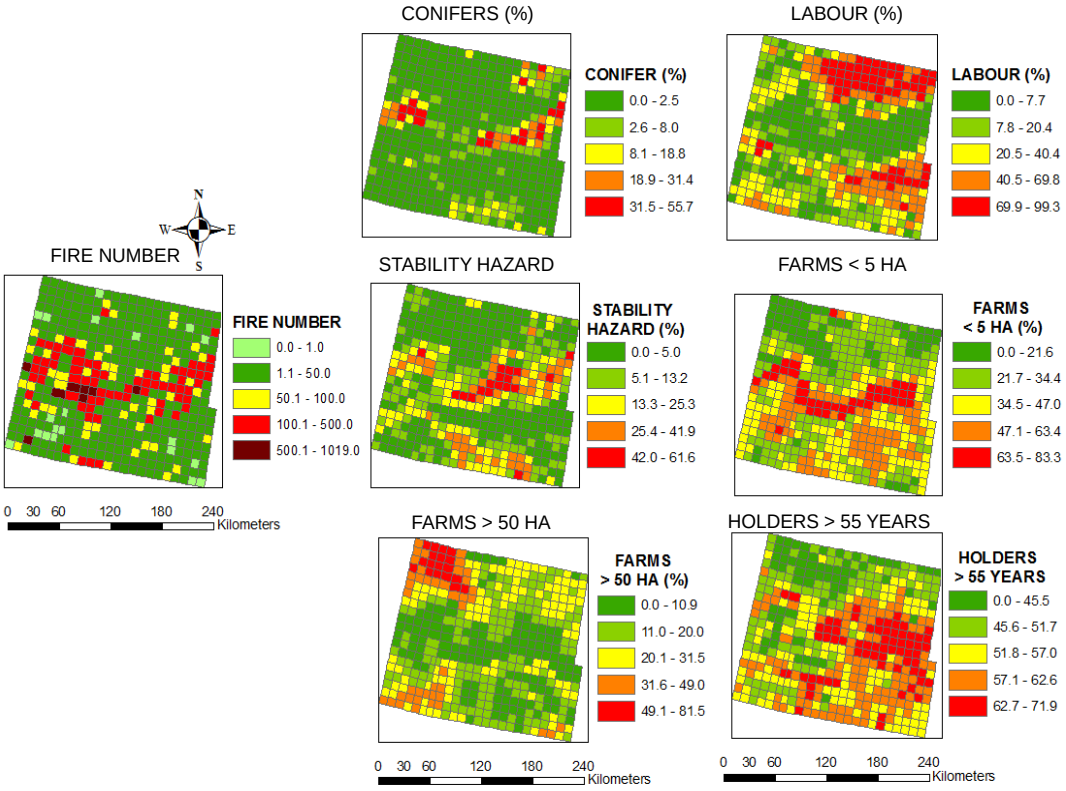

Figure 17. Maps of fire occurrence and of main driving factors spatially-explicit and aggregated by time (1974-2008) in the study area of Central Spain (by UCLM). Fire number: Sum of daily number of fires at cell scale (10 x 10 km) from 1974 to 2008. Source: Spanish Fire Statistics from the Ministry of Agriculture and Environment. Conifers (%): Mean percentage of occupation of conifer forests at cell scale (10 x 10 km) based on LULC maps from 1978-1986-2000-2006. Labour (%): Mean percentage of occupation in agriculture areas at cell scale (10 x 10 km) based on LULC maps from 1978-1986-2000-2006. Stability Hazard (%): Mean percentage of occupation of stable areas (no change areas) at cell scale (10 x 10 km) between pairs of LULC maps (1978-1986, 1986-2000 and 2000-2006). Farms < 5 ha: Mean density of small farms (< 5 ha) at cell scale (10 x 10 km) based on Agrarian Censuses from 1972-1982-1989-1999-2009. Farms > 50 ha: Mean density of large farms (> 50 ha) at cell scale (10 x 10 km) based on Agrarian Censuses from 1972-1982-1989-1999-2009. Holders > 55 years: Mean percentage of land-holders older than 55 years at cell scale (10 x 10 km) based on Agrarian Censuses from 1972-1982-1989-1999-2009.

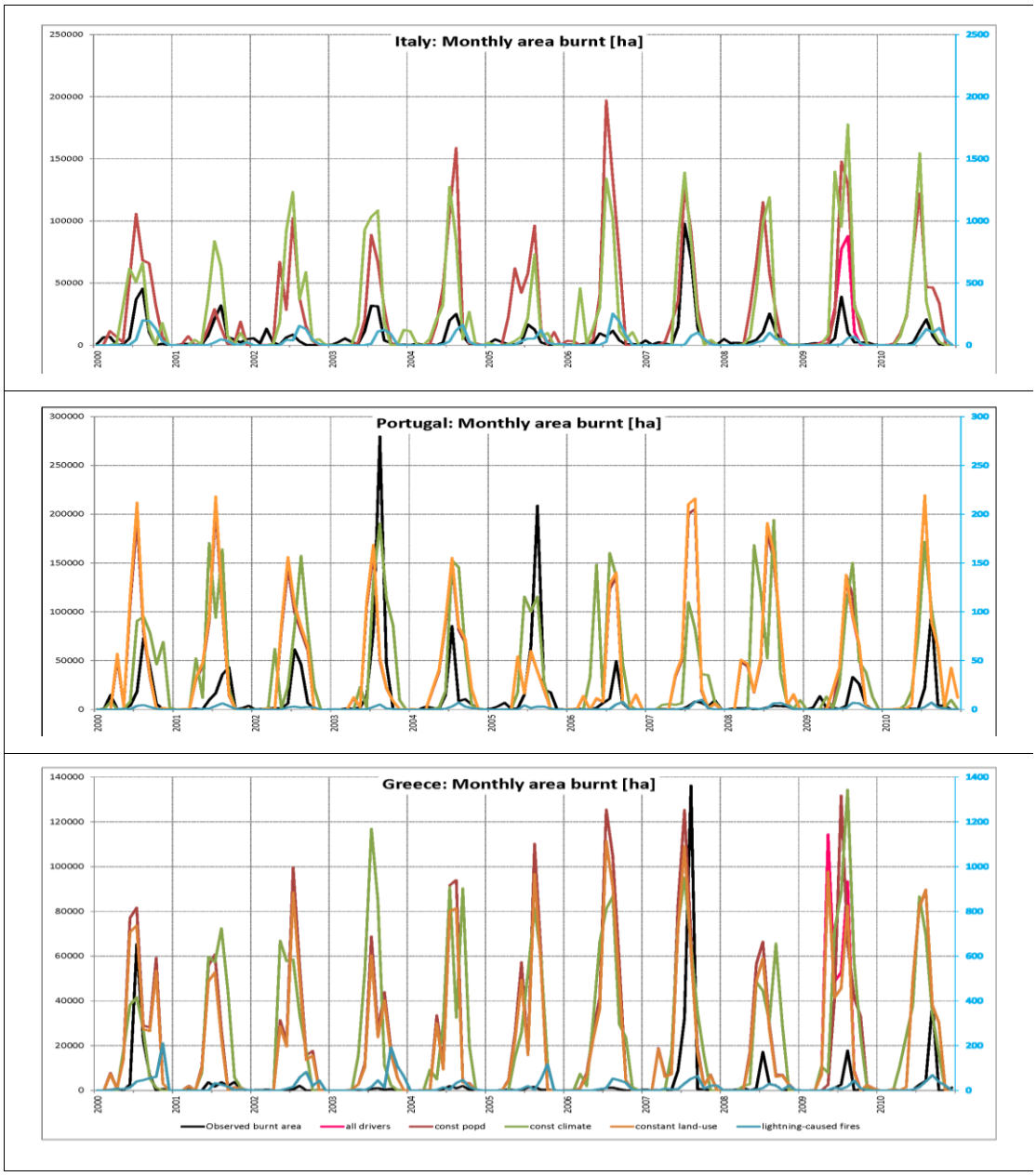

Figure 18. Monthly area burnt [ha] as simulated by LPJmL-SPITFIRE between 2000-2010. Results of factorial experiments (experiment 1 – "lightning-caused ignitions" on secondary axis; experiment 2 – "const popd", experiment 3 – "constant climate"; experiment 4 – "constant land-use"; experiment 5 – "all drivers") are shown for Italy (top panel), Portugal (central) and Greece (bottom panel) exemplarily. Observed burnt area (black line) is taken from the EFFIS data base.

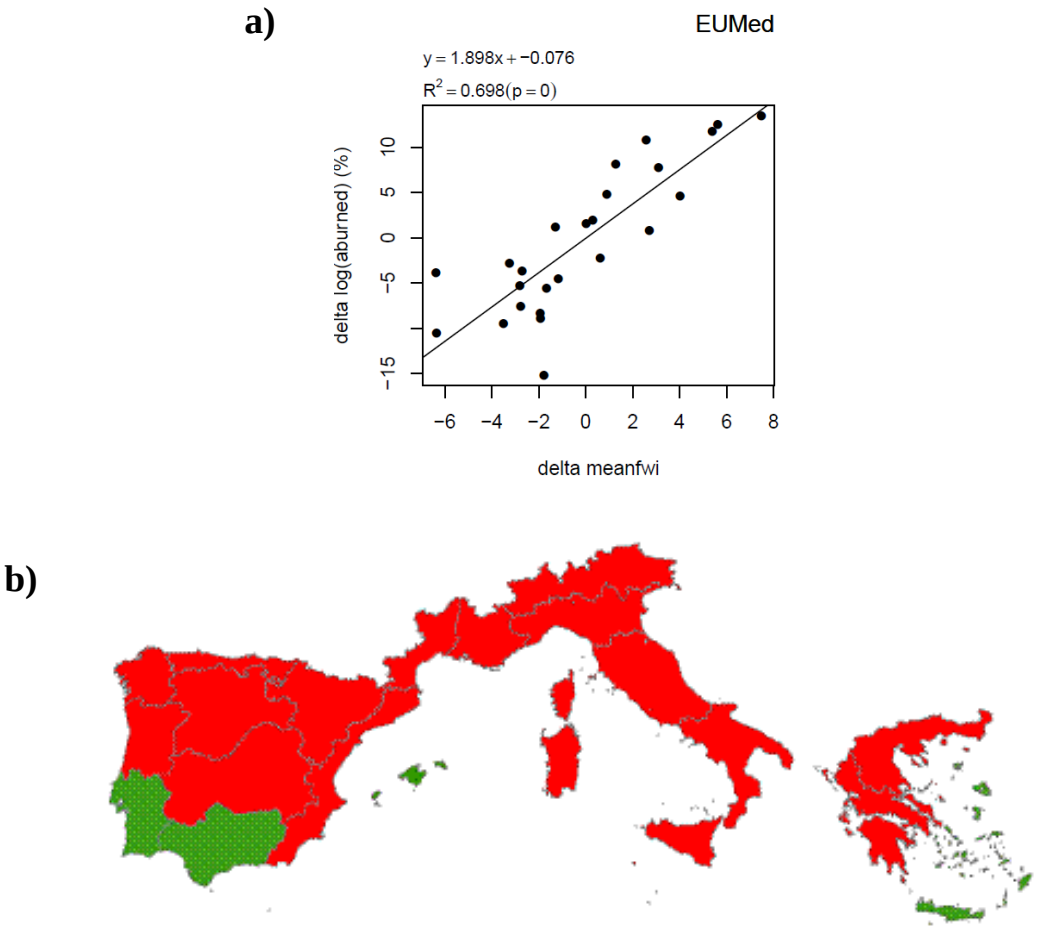

Figure 19. a) Model for all EUMed regions aggregated, showing the relationship between yearly relative change (%) in area burned as function of change in average FWI conditions in summer; b) EUMed regions with positive and significant relationships between the year-to-year change in number of fires (NF) or burned area (BA) as a function of year-to-year change in climate as reflected by the mean FWI index of the fire season. Positive relationships indicate that climate and fires were related during the studied period, under the assumption that on a year-to-year basis all other factors did not significantly change as to affect fires. Red: NF and BA significant; Green: only one relationship significant (NF or BA).

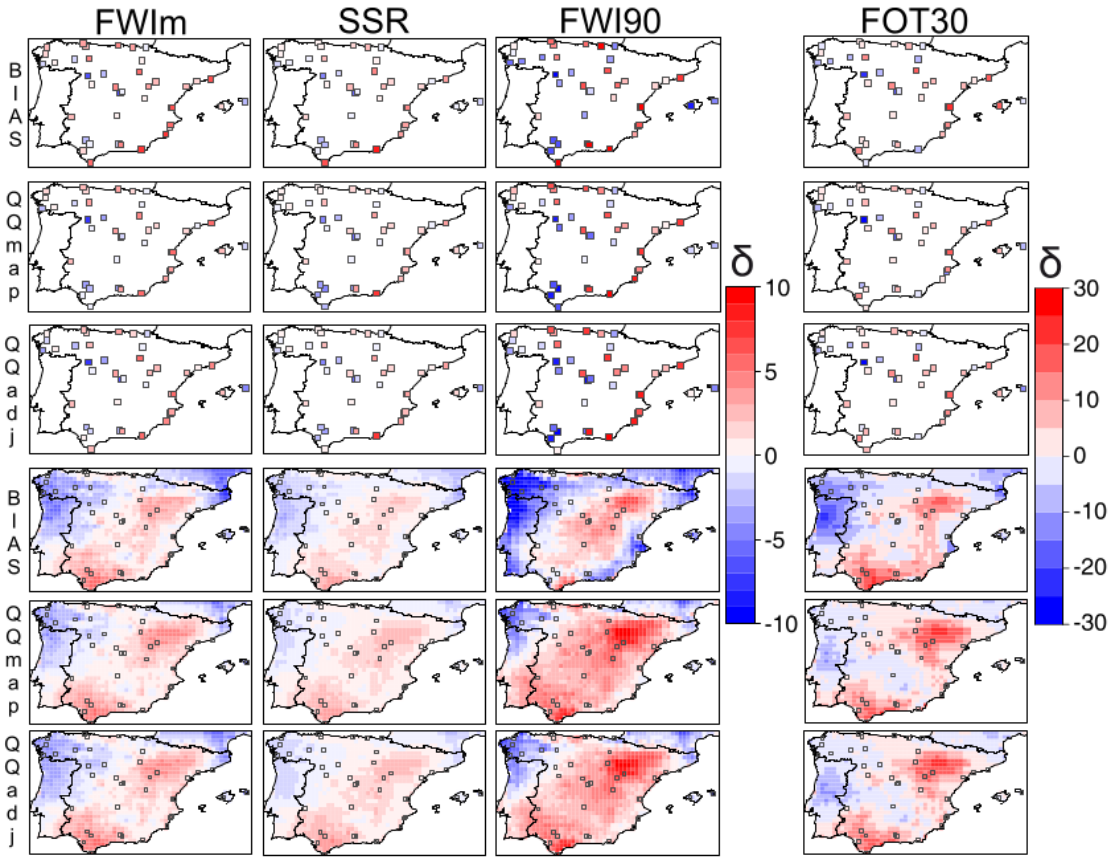

Figure 20. Results of the statistical correction of the WRF-B RCM projections for the fire danger indicators FWIm (mean Fire Weather Index), SSR (seasonal severity rating), FWI90 (90th percentile of FWI) and FOT30 (percentage of days with FWI>30), according to the three methods tested (simple bias correction 'BIAS', quantile-quantile mapping 'QQmap' and quantile-quantile adjustment 'QQadj') and using as observed control either WATCH (gridded) and AEMET (stations) datasets for the baseline period 1980-89. In the panels it is represented the difference (delta, δ) between the corrected scenarios and the observed SSR for the period of the projections (1990-99). In each panel, the mean absolute error (MAE) is indicated as a measure of the departure between the corrected scenarios and the corresponding observations. Note that MAE values indicated in upper case in WATCH correspond to the spatial mean of the whole domain, and in lower case is indicated the mean at the AEMET point locations. For details on the methodology applied see e.g., Amengual et al. 2012; Journal of Climate, 25: 939–957).

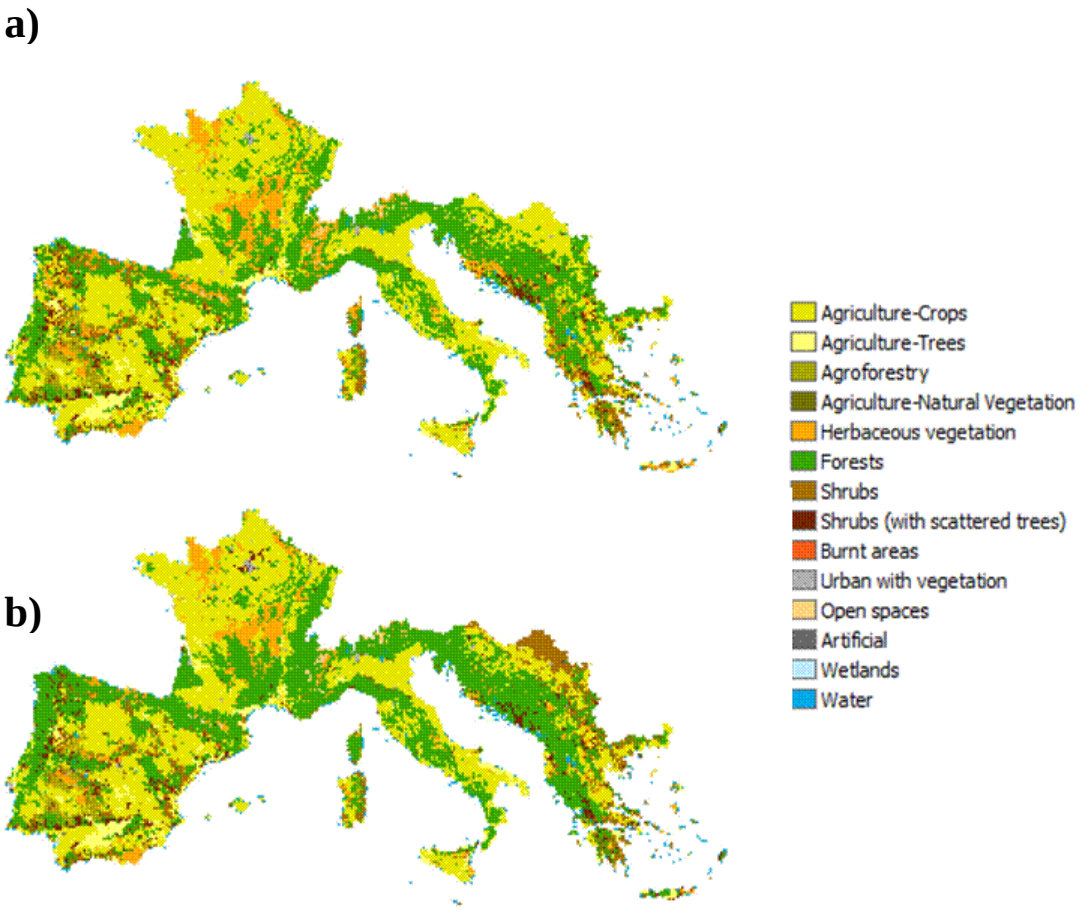

Figure 21. Modeling land use and land cover based on static or dynamic factors including climate (A1B), population density, land-demand (ICES, A1B) at a spatial resolution 5 min (ca. 10 km) a) year 2000 and b) year 2100.

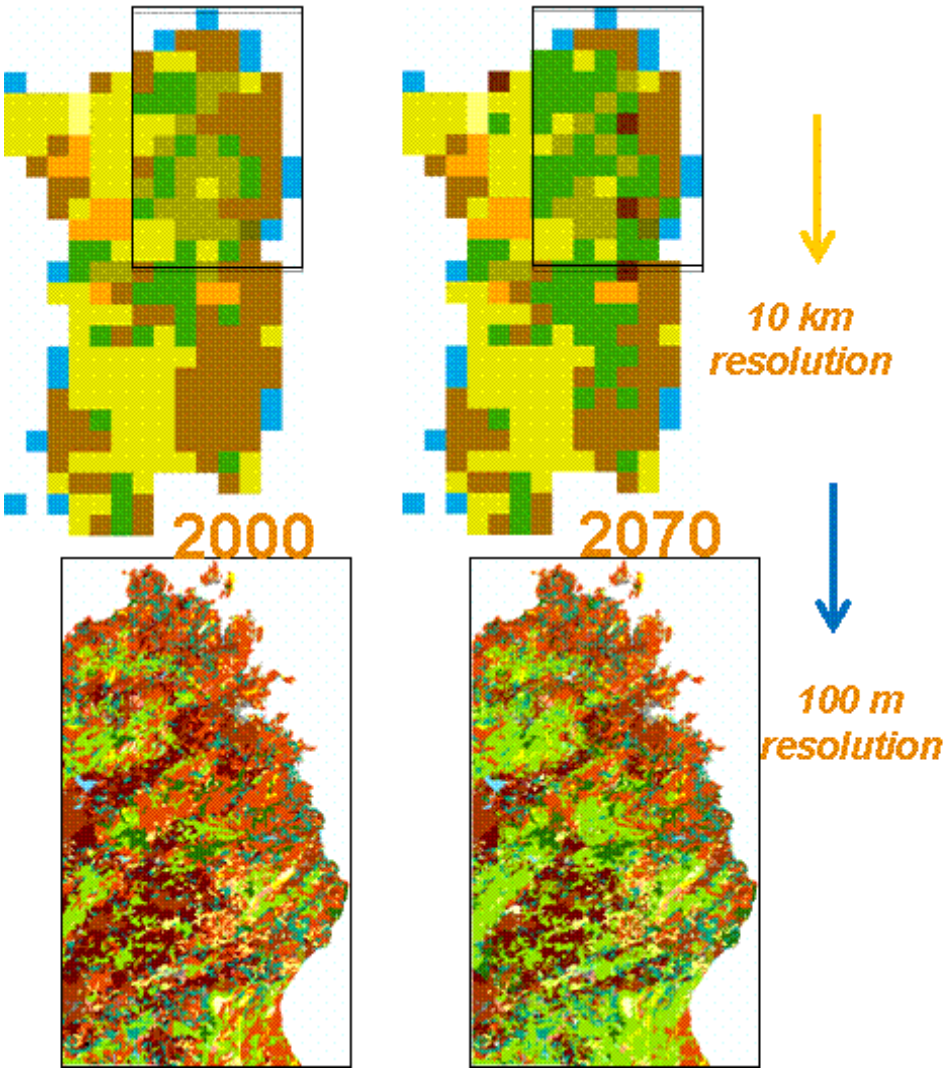

Figure 22. Downscaling LULC projections (LUC@CMCC) from 10 km to 100 m, appropriate for using fire simulators.

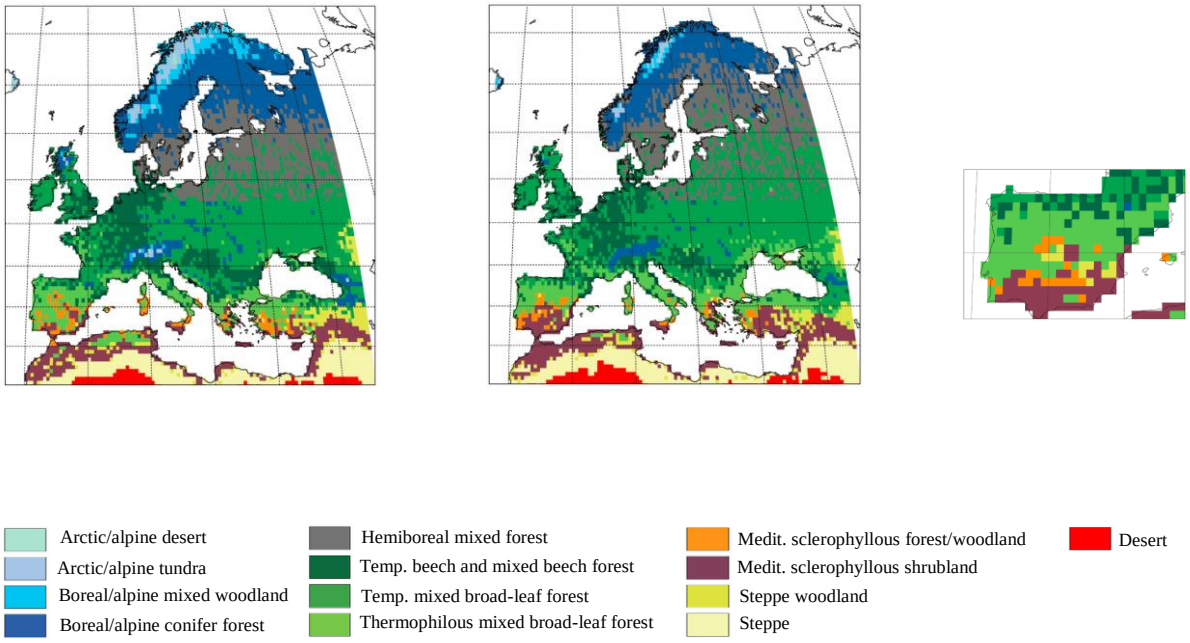

Figure 23. Modeled potential natural vegetation (PNV) in "full-effect" experiment present date (left panel, average 1981-2000), compared with future (right panel, average 2081-2100), and contrasted with (small inset) future without fire for the Iberian Peninsula averaged 2081-2100. Simulations were driven by MPI-ESM-LR, RCP 8.5 and SSP 5. Parameters of plant functional types and definition of biomes classes adopted from Hickler et al., 2012. Global Ecology and Biogeography, 21 (1): 50-63.

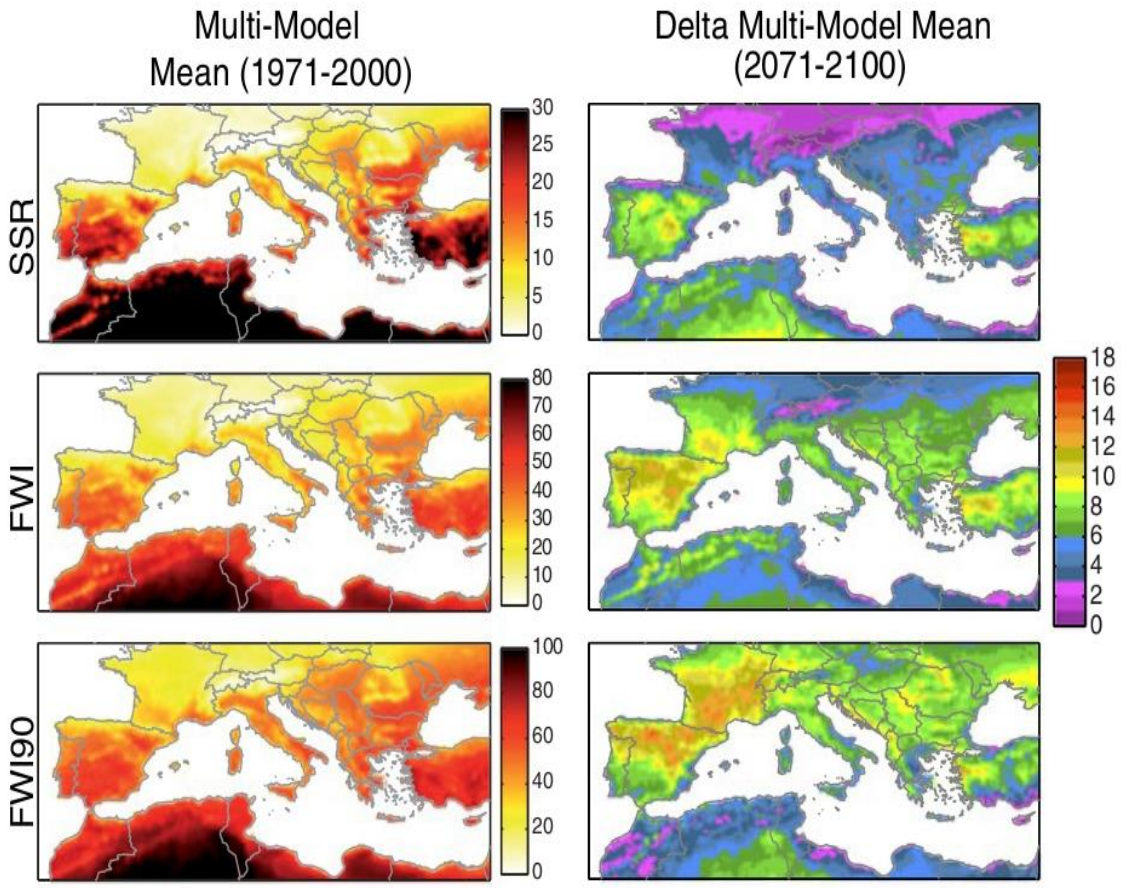

Figure 24. Control (1971–2000) and future projections (deltas, 2071–2100) of FWI, 90th percentile of FWI (FWI90) and seasonal severity rating (SSR) for the Mediterranean for the period 2071–2100 according to the multi-model ensemble of five RCM-GCM couplings from the EU-funded project ENSEMBLES, corresponding to the SRES A1B emissions scenario for the fire season (JJAS). Delta values (right panels) are calculated as the anomalies of the future scenario with regard to the multi-model ensemble mean of the current climate values (left panel) (from Bedia et al, 2014; Climatic Change, 122: 185-199)

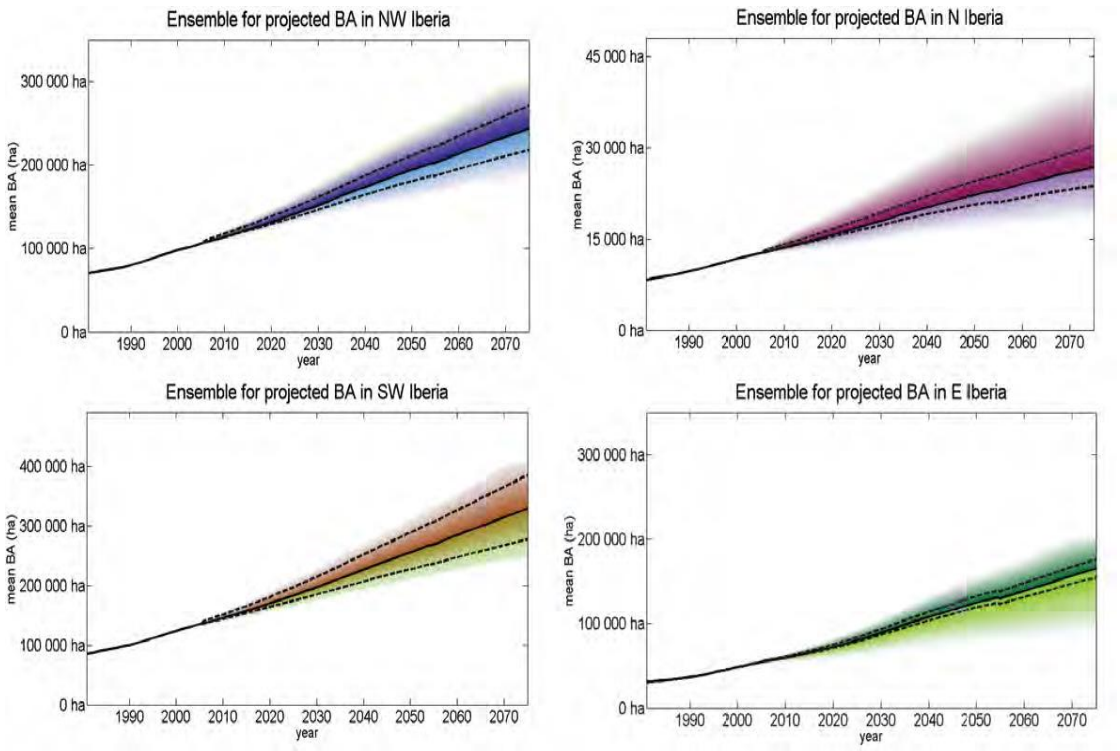

Figure 25. Ensembles of projected mean burned area (BA) for the period 1981-2075 in the four Iberian clusters. The solid line represents the mean of all 16 considered simulations. The upper dashed line represents the mean of the simulations that use fixed reference climatology, while the lower dashed line represents the mean of the simulations using moving reference climatology. Darker and lighter shades represent ensemble uncertainties of the previous simulations and where obtained using inter-quartiles. A 25-year moving average was applied to all series.

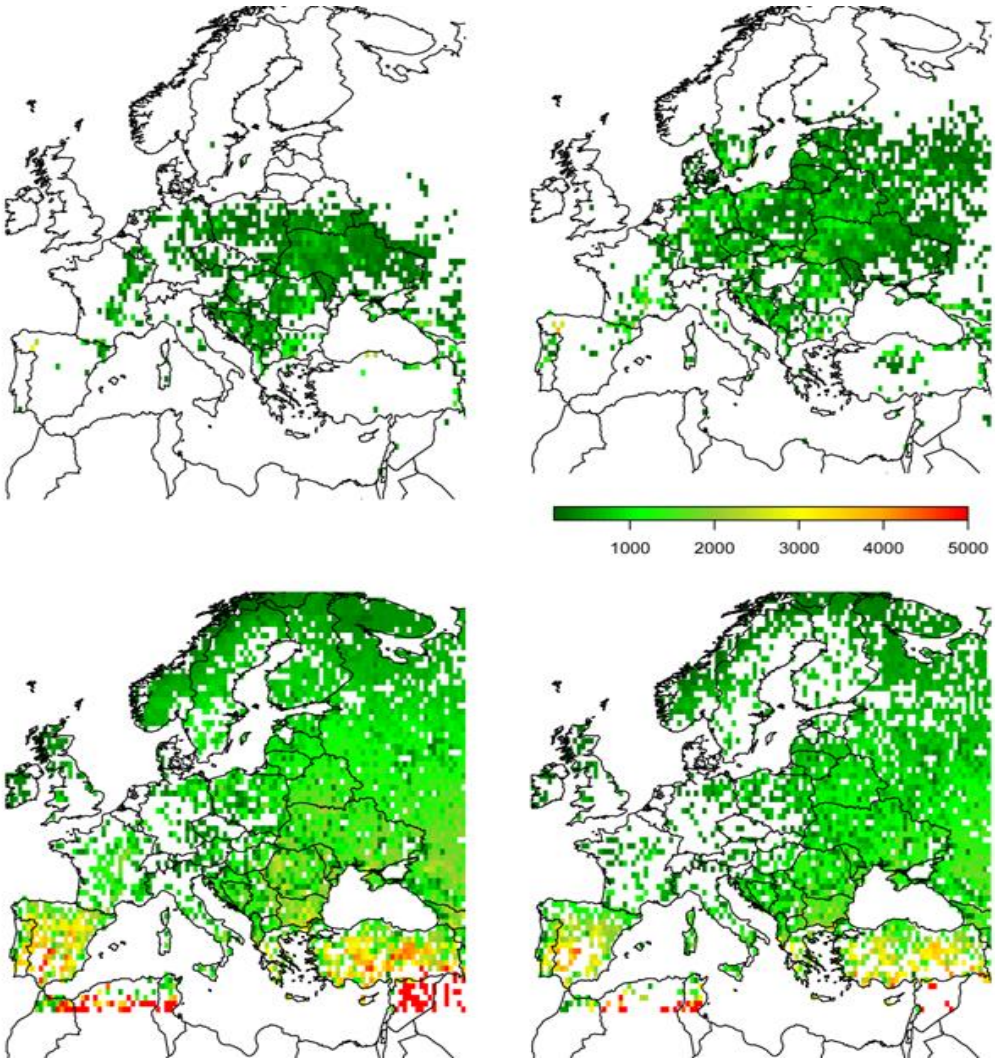

Figure 26. Average future burned area [ha] in regions identified as new fire-prone areas in Europe and Northern Africa. Simulations by the LPJmL-SPITFIRE model (top row) and the LPJ-GUESS-SIMFIRE model (bottom row) under the intense climate change scenario of the 5th IPCC report (RCP8.5-SSP5) from the HadGEM2 climate model (left column) and the CCSM climate model (right column).

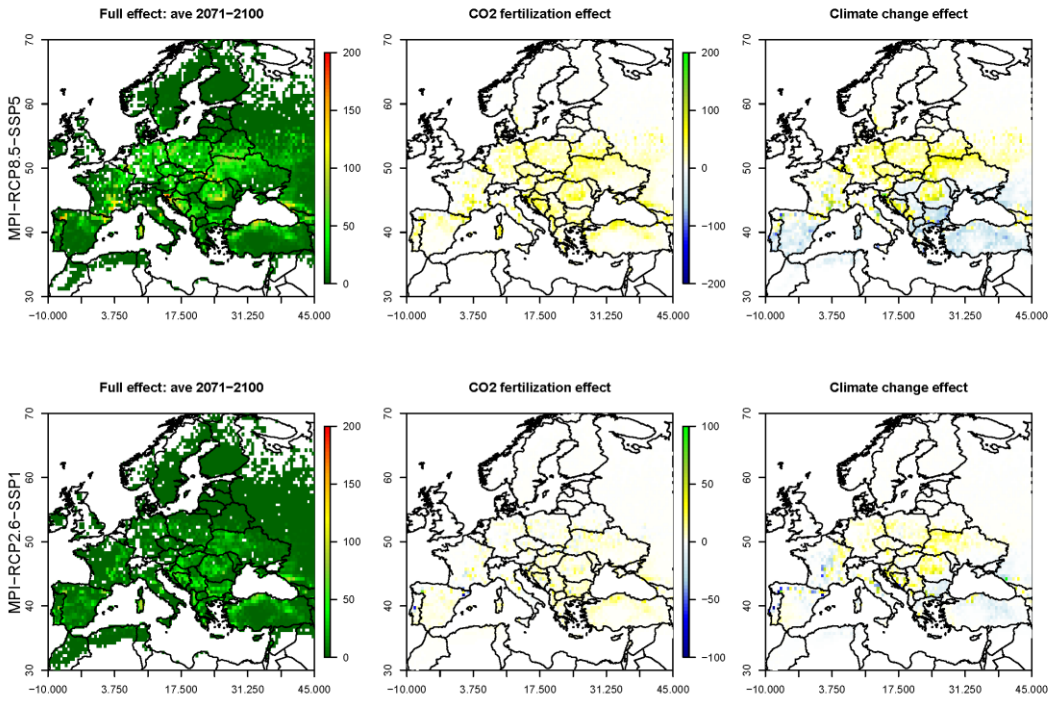

Figure 27. Future biomass burned by the end of the century (2071-2100) for low (RCP2.6) or high (RCP8.5) climate change and one GCM (MPI) and the LPJmL-SPITFIRE model, differencing the effects of CO2 and climate.

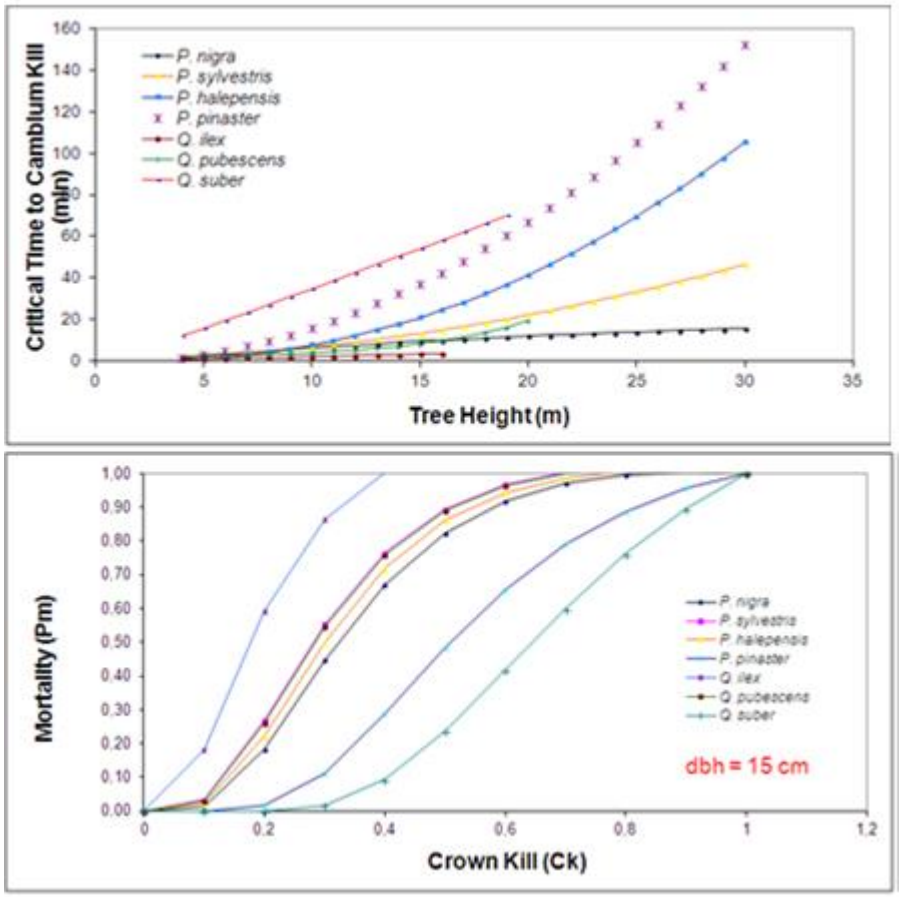

Figure 28. Variation of critical time to cambium kill (top) and predicted mortality rate (Pm) as a function of crown kill by fire (Ck) (bottom) for pine and oak species in Provence (France).

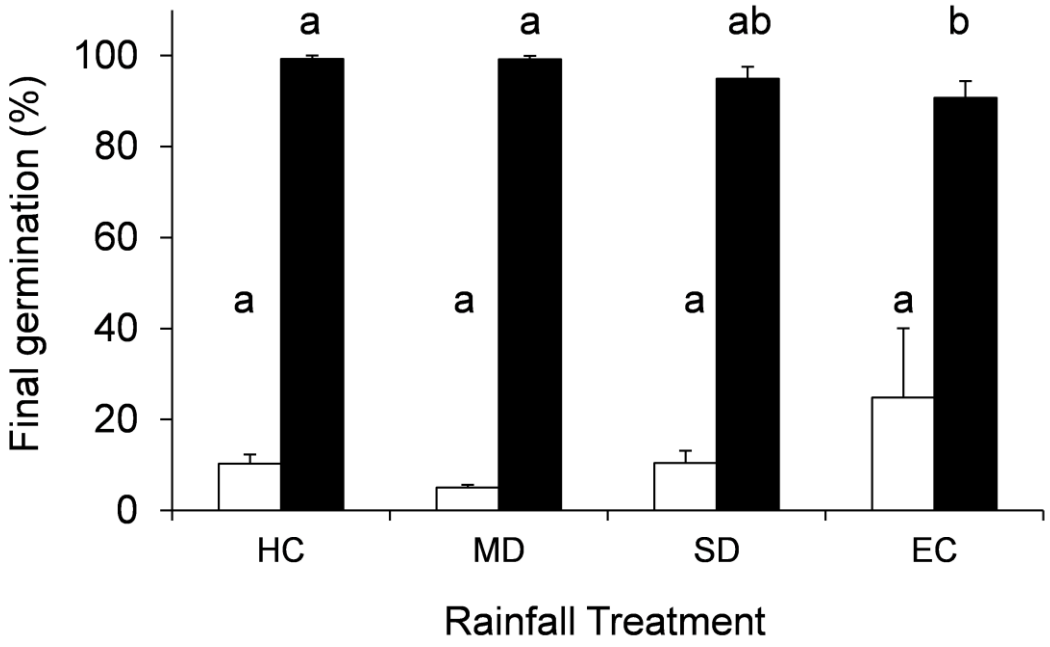

Figure 29. Final germination (%) of seeds of *Cistus ladanifer* from different rainfall manipulation treatments (EC: environmental control, HC: historical control, MD: moderate drought, SD: severe drought). Empty bars show FG of intact seeds and solid bars show FG of seeds exposed to heat-smoke treatment prior to germination. Letters show significant differences among rainfall manipulation treatments from pair wise comparisons with Bonferroni correction ($P \leq 0.05$).

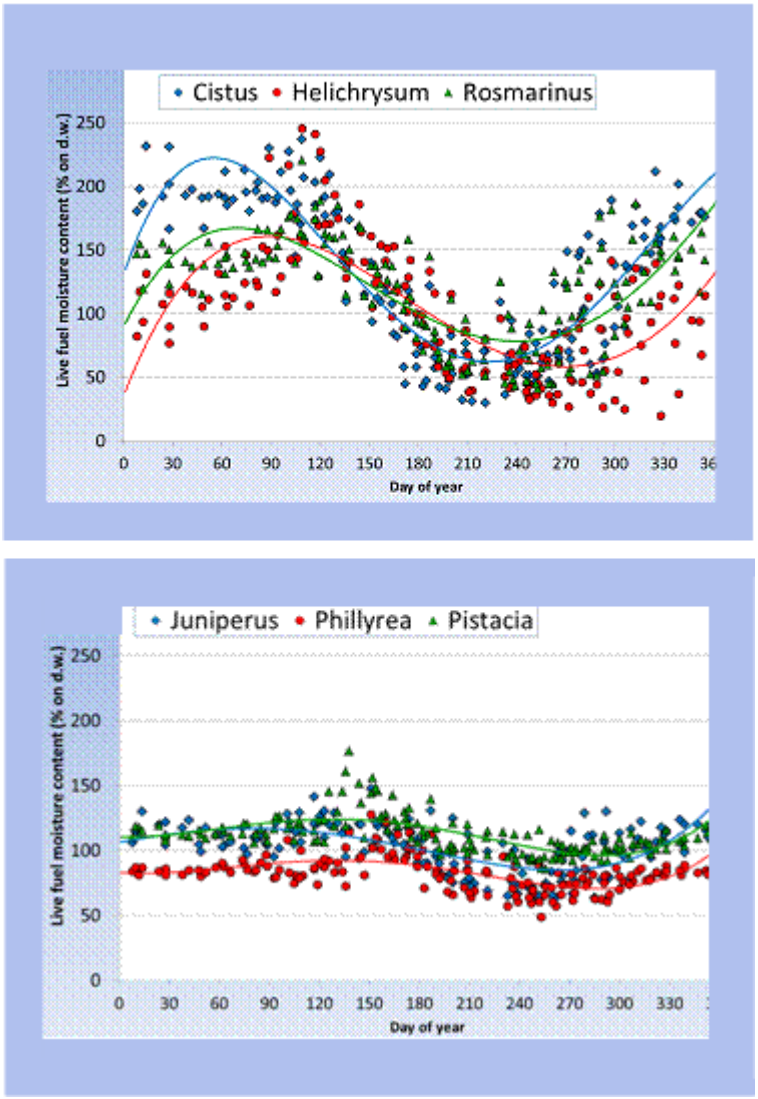

Figure 30. Fuel moisture content along the year for species that differ in their functional type. Note the differential response among malacophyls (top) and evergreens (bottom).

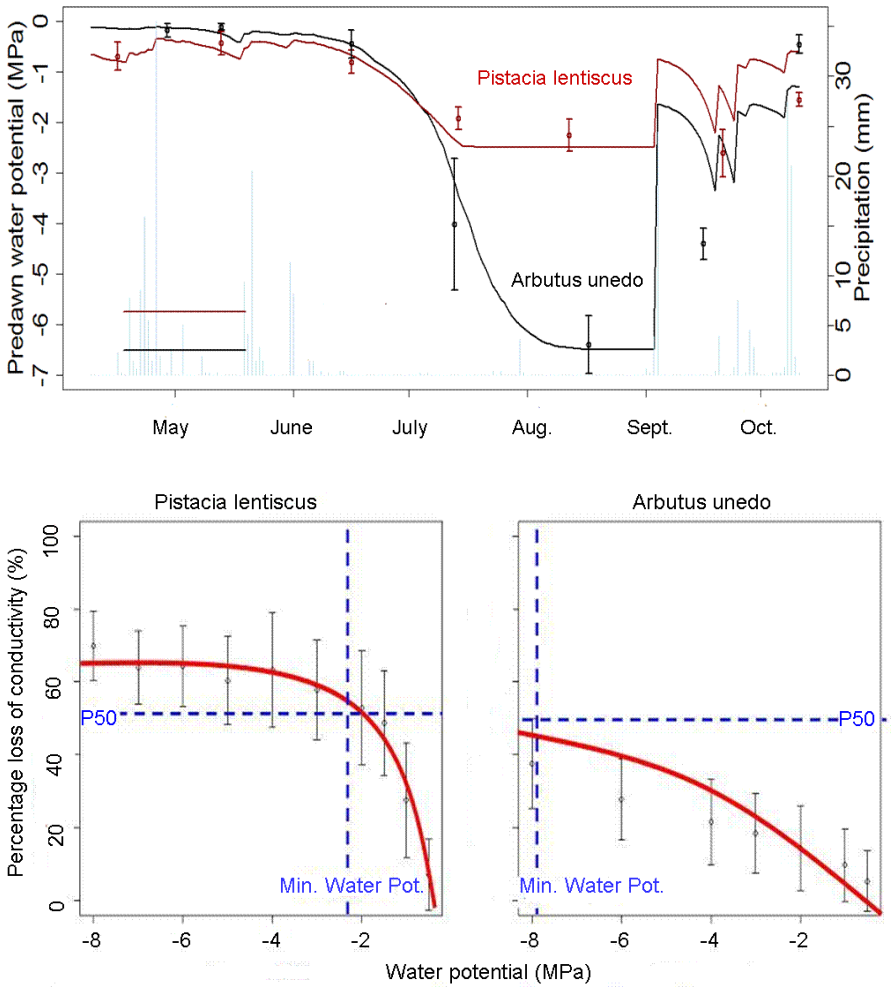

Figure 31. Seasonal course of predawn water potential for *Arbutus unedo* and *Pistacia lentiscus*, two species with contrasted water strategies (top). Percentage loss of conductivity as a function of water potential in the two species (bottom). Differential vulnerability to cavitation is measured by the percentage of conductivity lost according to water potential. 50% loss of conductivity (P50) corresponds to field measurements of minimum water potential observed during the season.

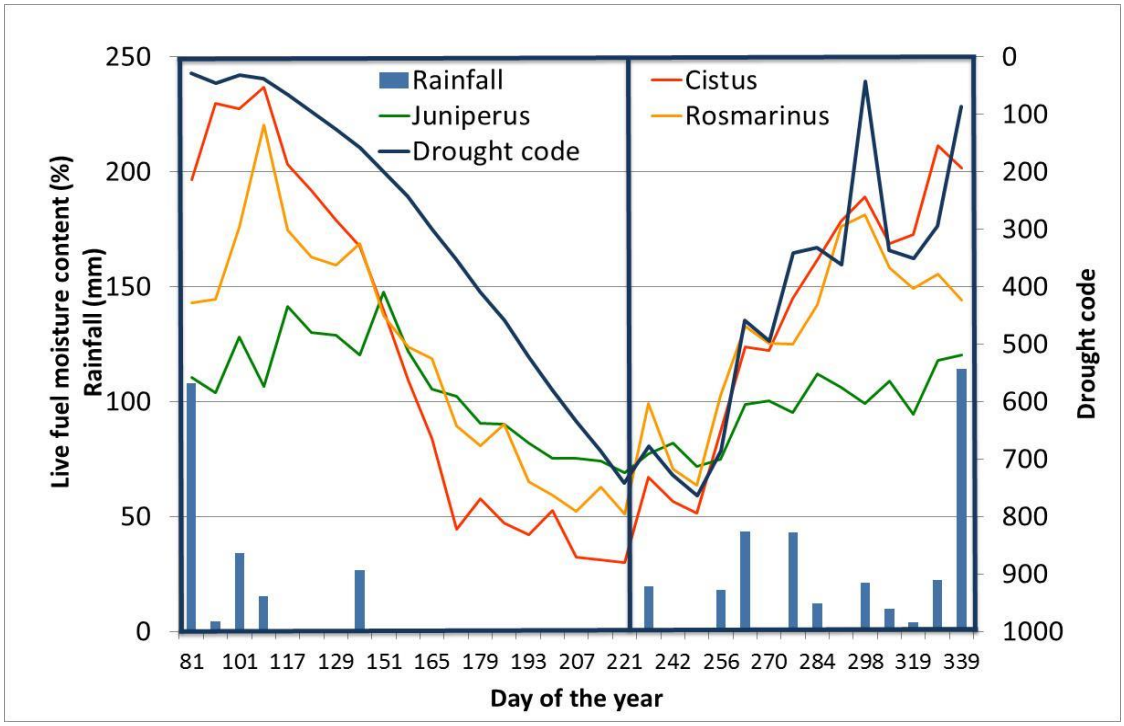

Figure 32. Variation of the drought code (DC) for different types of Mediterranean species with contrasted water holding strategies. This figure shows that in the falling phase of moisture content (winter to spring) DC was not close to the live fuel moisture content and rainfall. It correlated much better during the moisture raising phase (mid-summer to autumn), thus suggesting that DC is more appropriate to identify the end of fire danger season rather than the date of starting. In some species less sensitive to drought (e.g., *Juniperus*) live moisture content is weakly correlated with DC.

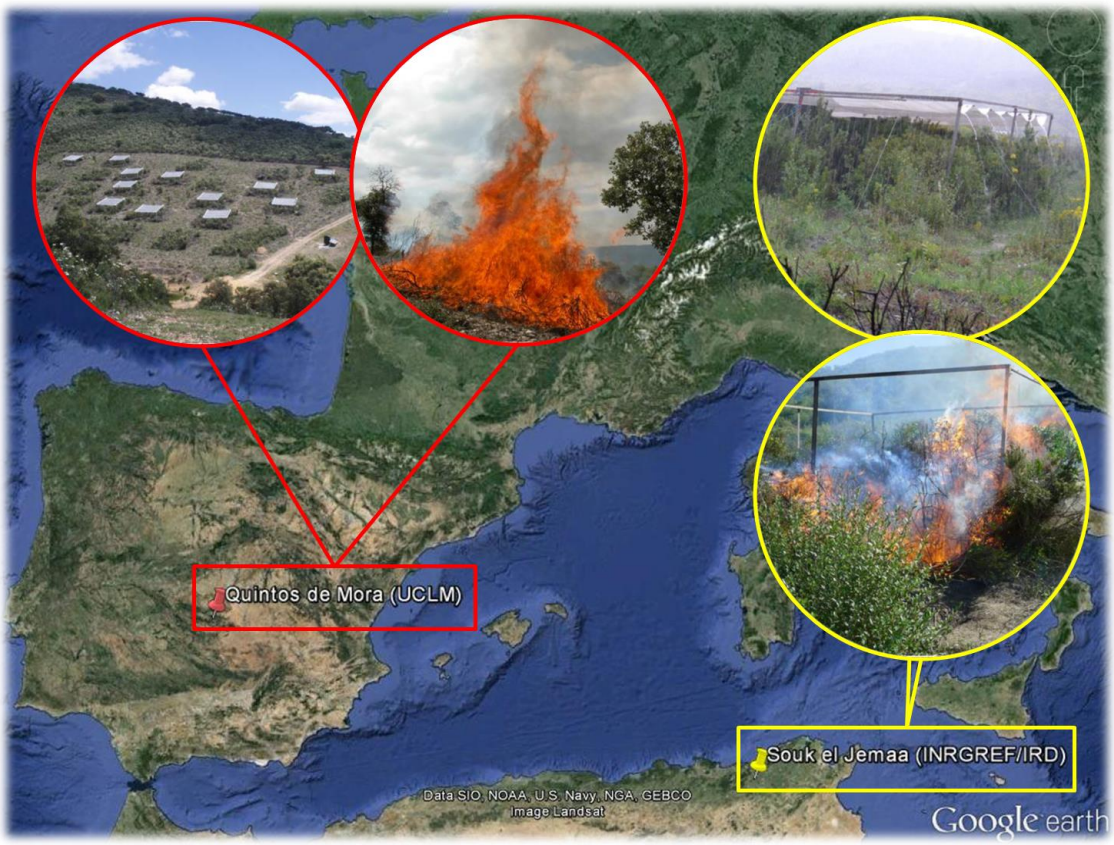

Figure 33. Location of the study sites and pictures showing the systems for rainfall manipulation experiments at Quintos de Mora (Toledo, Spain) and Souk el Jemaa (Tunissia) and experimental burning at both sites.

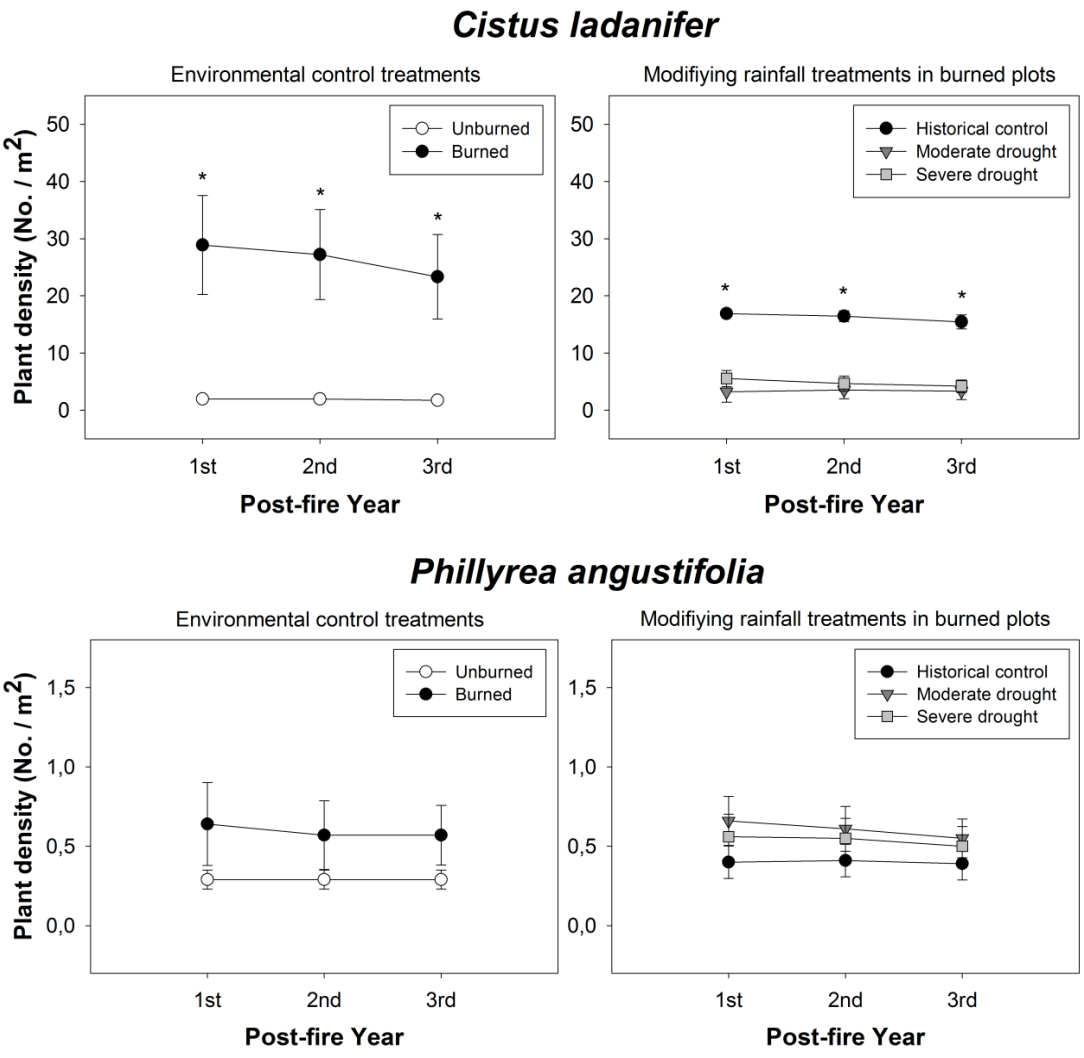

Figure 34. Plant density recorded in the different treatments for *Cistus ladanifer* (seeder) and *Phillyrea angustifolia* (resprouters) at the end of the 1st, 2nd, and 3rd year after fire. Asterisks represent statistically significant differences among treatments ($P \leq 0.05$).

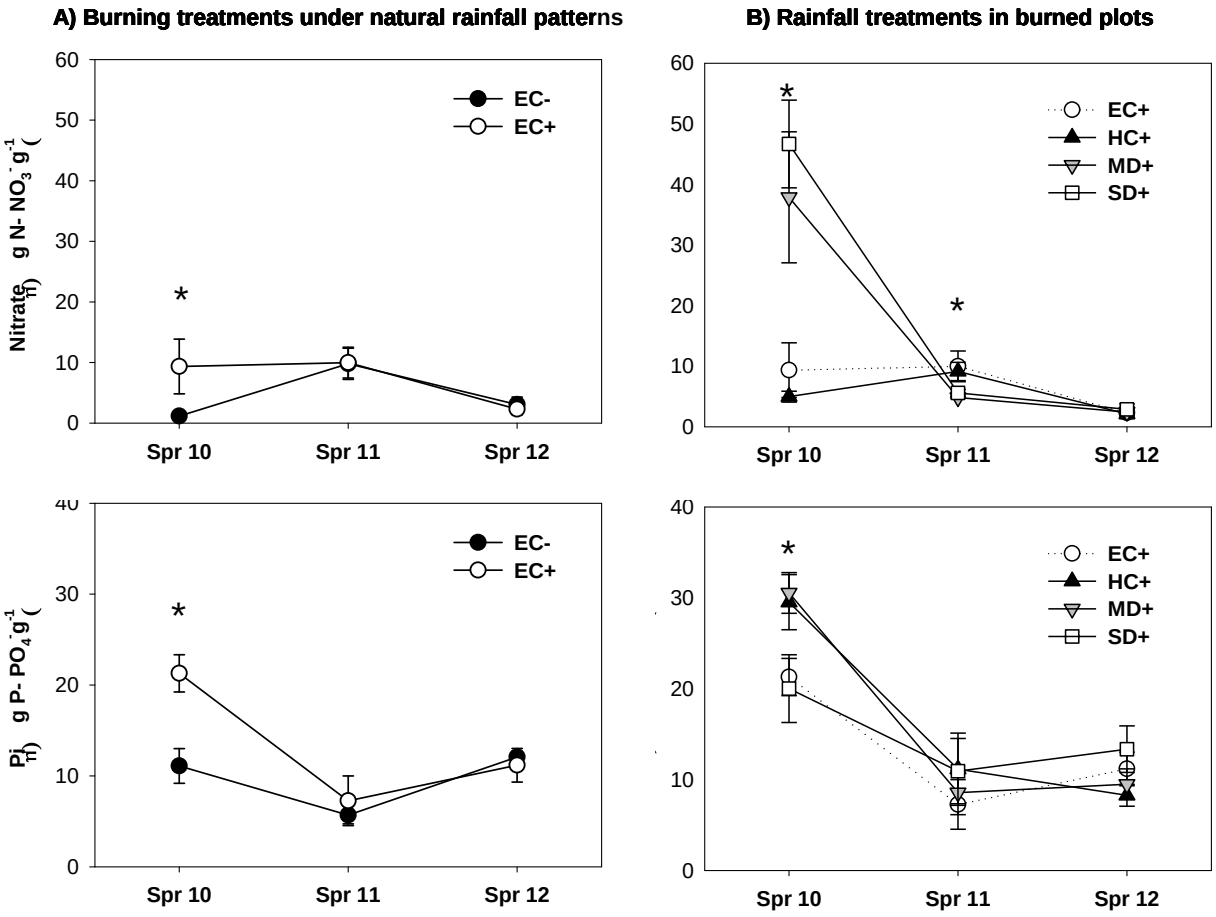

Figure 35. Soil concentration of nitrate and inorganic phosphate in the three springs after fire (2010, 2011 and 2012). Means are given ± SE. * indicate significant differences between burning treatments under natural rainfall patterns (A) or among different rainfall treatments in burned plots (B) ($P \leq 0.05$).

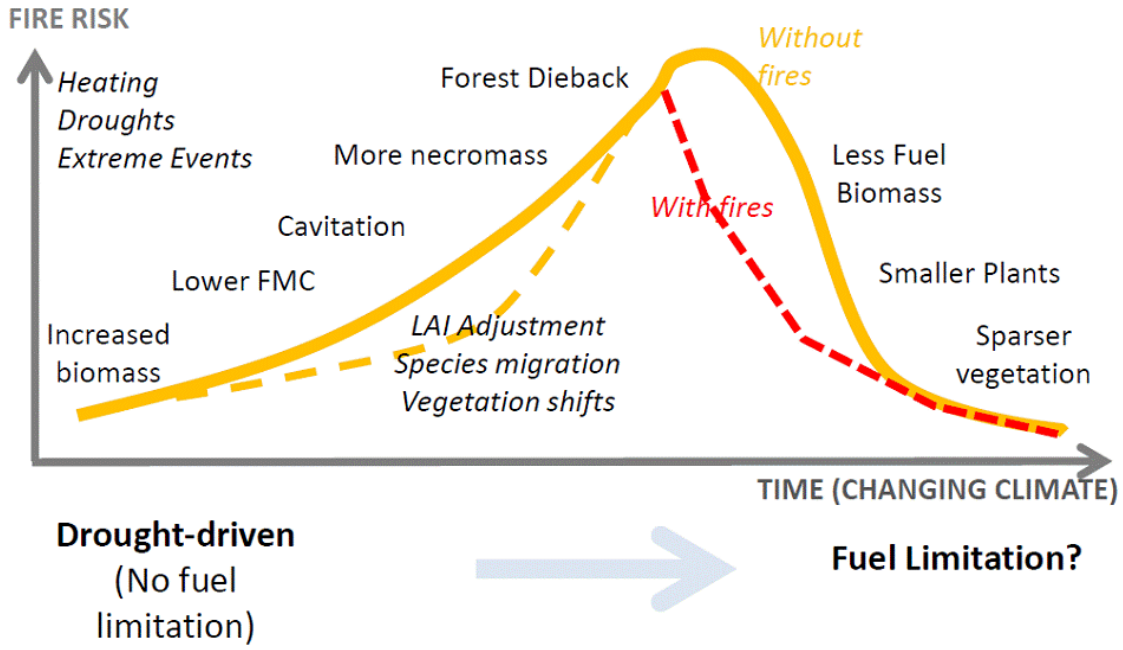

Figure 36. A possible model for future fire risk in Mediterranean fertile environments (such as France, Spain, or Italy) indicates that fire could shift from drought-driven as today (i.e., fires depend mostly on fire weather since fuel biomass is sufficient) to increased fire occurrence or intensity during several decades due to climate change (mitigated by different adaptive strategies of vegetation), then to fuel-limitation in the long-term because vegetation will decrease in biomass and become sparser. The leaf area index (LAI) characterizes the extent of a species canopy.

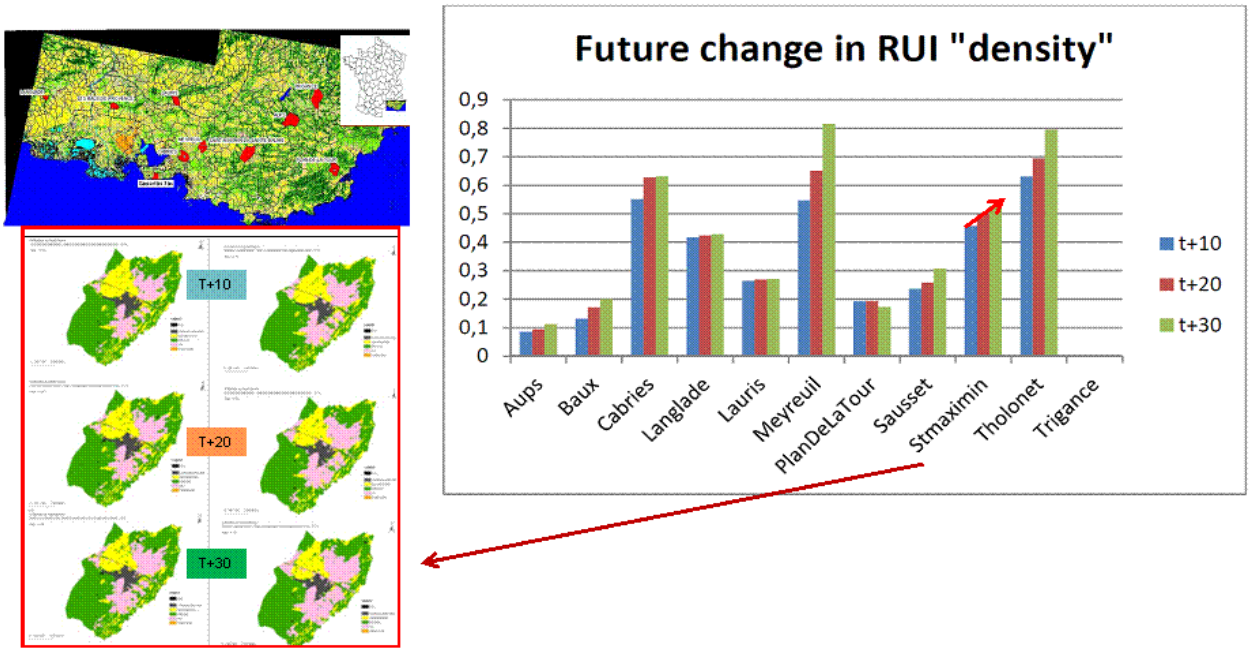

Figure 37. Modeling changes in the RUI in 11 areas in southern France: % RUI of total area in the next 30 years.

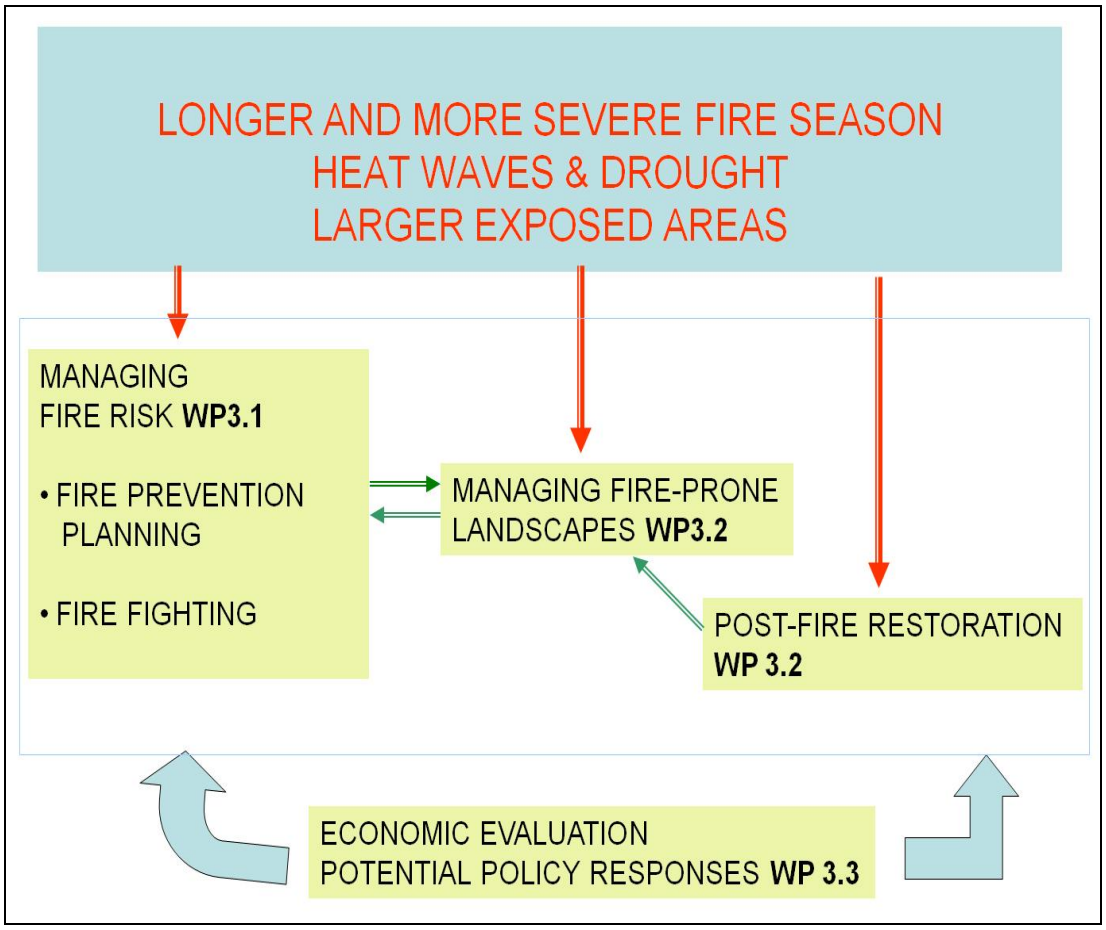

Figure 38. Module 3: structure and interrelations between tasks.

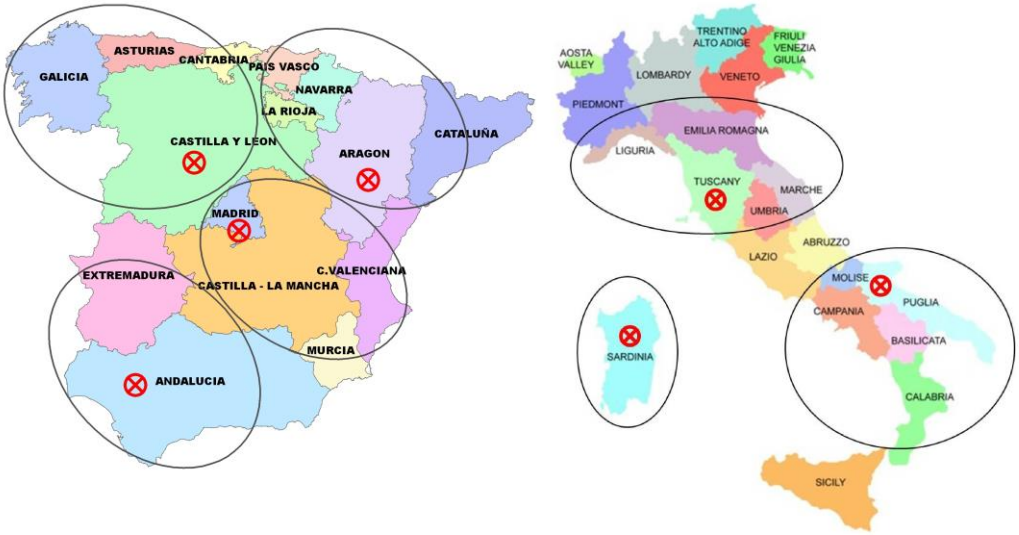

Figure 39. Map showing locations of stakeholders meetings in Spain and fire managers operations meeting in Italy.

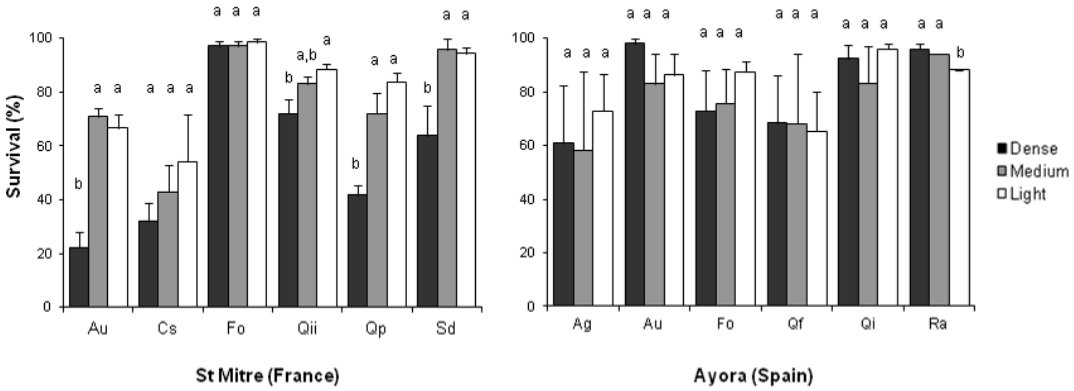

Figure 40. Species survival under dense canopy cover (black bars), medium canopy cover (grey bars) and light canopy cover in the 2 sites. Values correspond to species survival after 4 years in St Mitre and after 2 years in Ayora. Values are means of 4 (St Mitre) or 3 (Ayora) plots per treatments; error bars represent the standard deviation. Different letters indicates differences between treatments for one specie (Tukey post-hoc test, $P \leq 0.05$). Species code are: *Arbutus unedo* (Au), *Fraxinus ornus* (Fo), *Ceratonia siliqua* (Cs), *Quercus ilex ilex* (Qii), *Quercus pubescens* (Qp), *Sorbus domestica* (Sd), *Acer granatense* (Ag), *Quercus faginea* (Qf), *Quercus ilex ballota* (Qi), and *Rhamnus alaternus* (Ra).

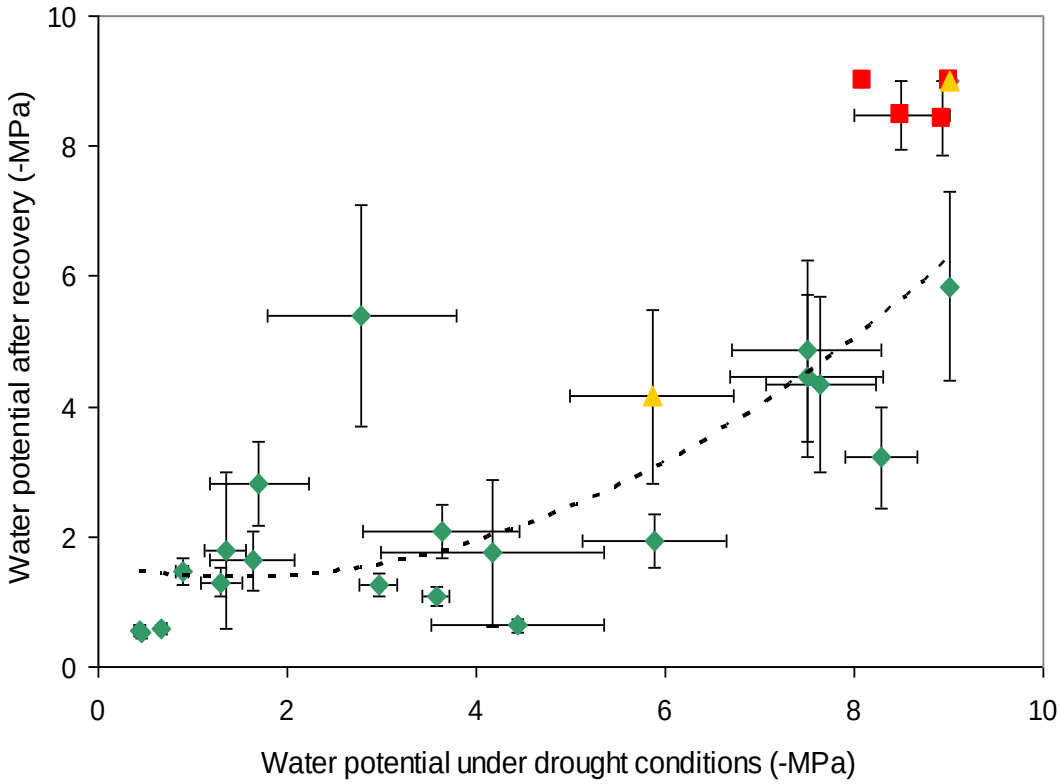

Figure 41. Relationship between water potential during the drought period and after rewatering (one month later). Red dots correspond to groups of dead plants (100% mortality) recorded one month after recovery. Yellow dots are plants with more than 50% of mortality. Studied species were: *Cistus albidus, Rosmarinus officinalis, Arbutus unedo, Quercus ilex, Fraxinus ornus*, and *Acer granatense.*

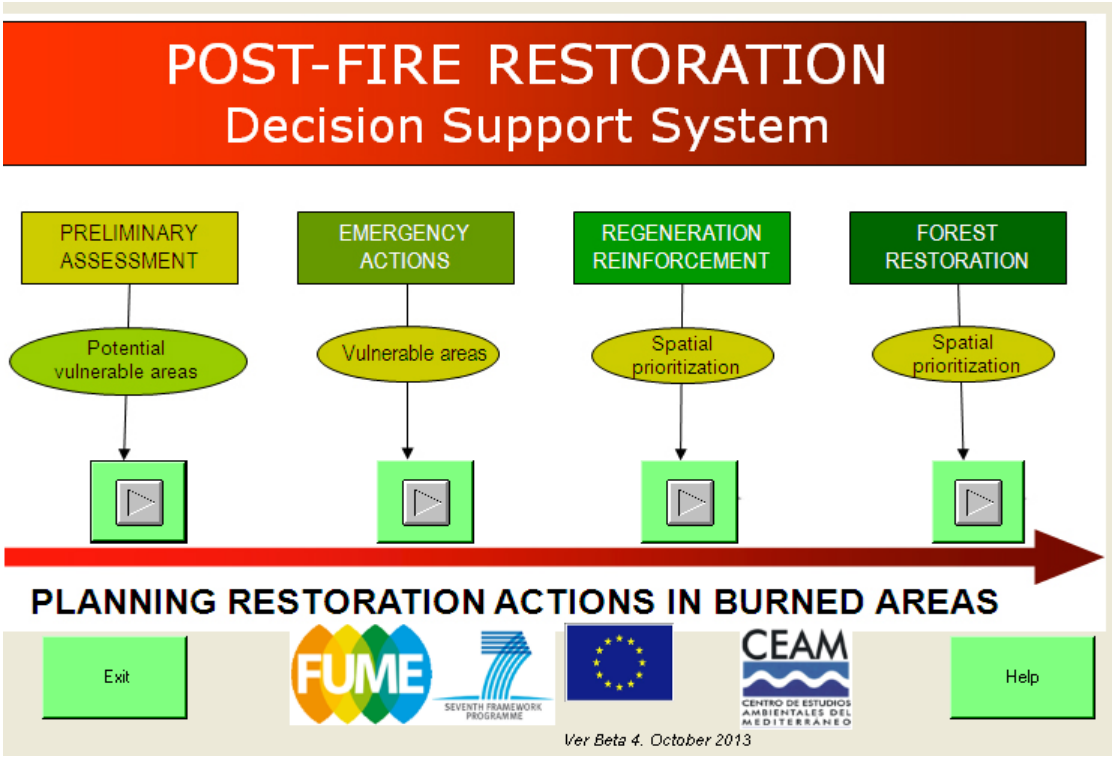

Figure 42. Managing societal response to future fire risk conditions.

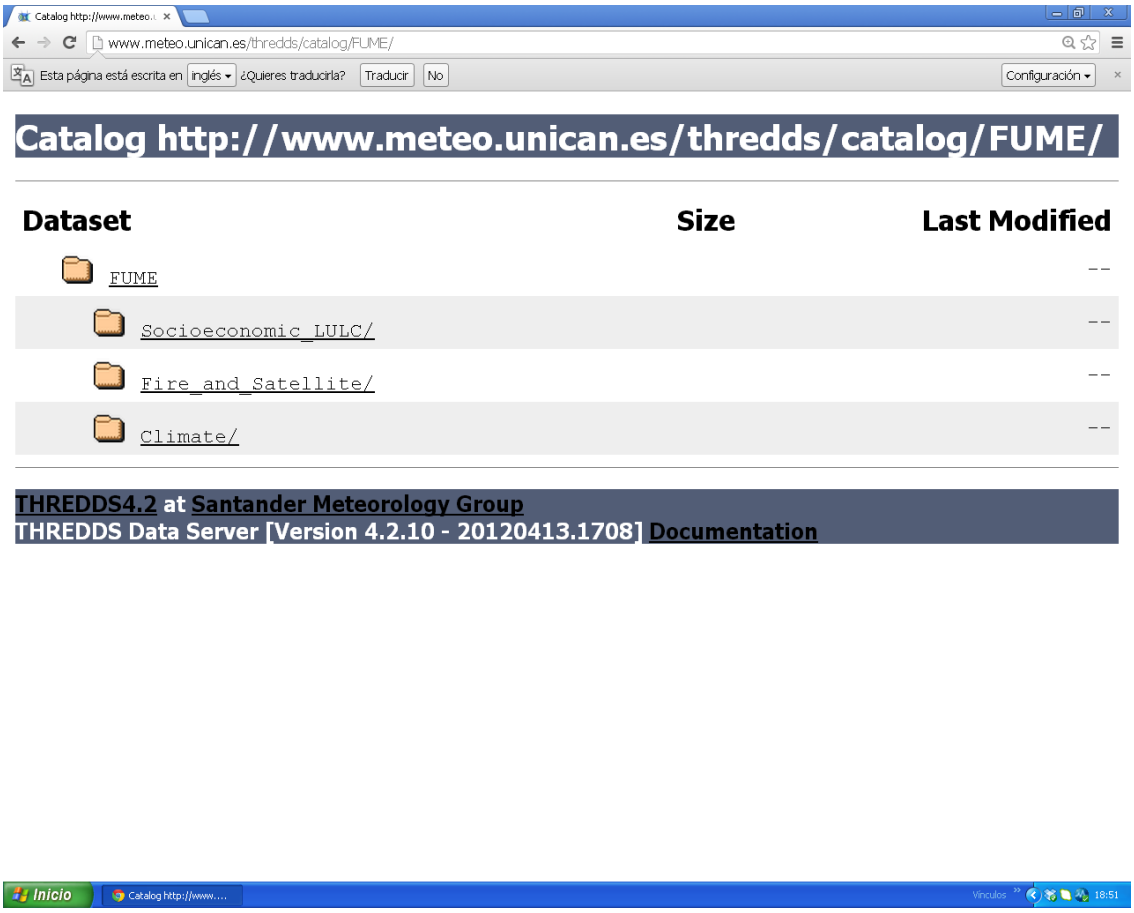

Figure 43. FUME-THREDDS Data Server, a web server intended for earth system data, that provides metadata and data access for scientific datasets, using OPeNDAP, HTTP and other remote data access protocols. Accessible without credentials at:

http://www.meteo.unican.es/thredds/catalog/FUME/

Figure 44. Location of the experimental and observational sites included in the FUME sites network.

Table 1. List of the study sites, at different scale, for each task of the three WP in Module 1.

	Landscape composition and structure dynamics,	***Mapping fires and evaluating fire regimes and***	***Assessing burned landscape features and the***	***The dynamics of the Rural Urban Interface (RUI)***	***Current relationships between fire and climate***	***Analysis of extremes conducive to extreme fire***	***Chief drivers for fire propagation at the***	***Recent contribution of observed climate change to***	***Recent role of socio-economic factors on fire***	***Integrated analysis climate change and socioeconomic change***
TASK	**1.1.1**	**1.1.2**	**1.1.3**	**1.1.4**	**1.2.1**	**1.2.2**	**1.2.3**	**1.3.1**	**1.3.2**	**1.3.3**
EUMed scale	x		x		x	x	x	x	x	
National scale										
Portugal		x			x	x				x
Spain		x			x	x		x		x
France		x								
Italy		x			x				x	
Greece	x	x	x		x	x		x	x	x
Turkey		x								
Finland					x	x				x
Regional scale										
Continental Portugal			x							
Central Spain	x		x						x	x
Eastern Spain	x									
Comunidad Valenciana (Spain)					x	x				
Autonomous Community of Madrid (Spain)	x		x						x	x
Provence (France)	x		x							
Languedoc-Roussillon (France)					x				x	
Sardinia (Italy)	x			x	x					
Tuscany (Italy)					x					
Peloponnese (Greece)	x				x	x			x	x
Attica (Greece)	x		x		x	x				
Antalya (Turkey)	x		x		x				x	
North Morocco					x					
Wester Cape (South Africa)					x					
Central and South-Central Chile	x	x			x					
Local sites										
Vall de Gallinera (Spain)	x						x			

Valle de Gredos (Spain)	x									
Aix-Marseille (Provence, France)							x			
North East Sardinia (Italy)				x						
North West Sardinia (Italy)				x						
Nuoro (Sardinia, Italy)							x			
Budoni (Sardinia, Italy)							x			
Alexandroupoli (Greece)							x			
Penteli (Greece)							x			
Attica (Greece)	x						x			
Mt Parnitha and Mt Penteli (Greece	x				x	x				

Table 2. Main characteristics of the study cases in Task 1.3.2 and statistical approaches.

Mediterranean and national scales						
Study area	**Partner**	**Spatial unit**	**Time period/s**	**Explanatory variables**	**Fire data source**	**Statistical approach**
EUMed *	JRC	10x10 Km grid	1988-1993, 1998-2003 and 2004-2009	Socio-economic + LULC	European Fire database	Ordered regression models
Greece	UOI	National NUTS3	1920-today 1951- today	Socio-economic	National fire statistics	Linear regressions and PCA ordinations
Italy	CMCC	National and geographical macro-areas	2000-2008	Socio-economic + weather	European Fire database and National fire statistics	Fixed and random effects panel econometric models
Regional scale						
Greece						
Peloponnese	UOI	NUTS5	1951-today	Socio-economic	National fire statistics	Linear regressions and PCA ordinations
Spain						
Central Spain	UCLM	10x10 Km grid	1974-2008	Socio-economic + LULC	National fire statistics	Zero-Inflated Negative Binomial models
Madrid region	CSIC	1x 1Km grid	1985-1987, 1991-1995, 2001-2005 and 2007-2010	Socio-economic + LULC	Fire perimeters from Landsat images	Poisson regression model
France						
Languedoc Roussillon	IRD	1x 1Km grid	1989-2006	Socio-economic + LULC+ weather + topography	National fire statistics	Boosted regression trees
Turkey						
Antalya	SAFRI	NUTS3	1980-2010	Socio-economic	National fire statistics	Panel data

* Includes: Portugal, Spain, Southern France, Italy and Greece.

Table 3. Factors significantly affecting the vegetation in Sierra de Gredos (*) in relation to years since last fire (YSLF), fire recurrence and interval.

Variable	YSLF	Recurrence	Interval
Cover			
Total	*		
Woody species	*		*
Herbaceous species		*	**
Species richness			
Total	**		*
Woody			
Herbaceous	**		*
Herbaceous diversity			
H Shannon	*		
Whittaker index		*	